

Polymerization of Acrylates with MAO Activated Iron(II) Complexes

Pascal Castro

Laboratory of Inorganic Chemistry
Department of Chemistry
Faculty of Science
University of Helsinki
Finland

Academic Dissertation

To be presented with the permission of the Faculty of Science of the University of Helsinki, for public criticism in the auditorium A110 of Chemicum, A.I. Virtasen Aukio 1, on 20th of June, 2005, at 12 noon.

Supervisors

Professor Markku Leskelä
and
Docent Timo Repo
Laboratory of Inorganic Chemistry
Department of Chemistry
University of Helsinki
Finland

Reviewers

Professor Tapani Pakkanen
Department of Chemistry
University of Joensuu
Finland

Docent Ari Lehtonen
Department of Chemistry
University of Turku
Finland

Opponent

Professor Bernhard Rieger
Inorganic Chemistry II
University of Ulm
Germany

© Pascal Castro 2005
ISBN 952-91-8875-7 (printed version)
ISBN 952-10-2520-4 (pdf)
<http://ethesis.helsinki.fi>
Yliopistopaino
Helsinki 2005

Abstract

A great deal of interest has been devoted to transition metal-mediated polymerization of (meth)acrylate monomers during the past fifteen years. The introduction of highly active homogeneous single-center transition metal catalysts has permitted impressive control over polymer microstructure, stereoregularity and molecular weight characteristics. Among the various transition metal based catalytic systems used for the polymerization of (meth)acrylates, the combination of a late transition metal complex with an alkylaluminum activator, for instance methylaluminumoxane, provides a robust, easily accessible, highly active catalyst. However, little is known about the exact nature of the catalytically active species formed during the activation process, as well as about the polymerization mechanism, *i.e.* initiation, propagation and termination steps.

In this thesis, methylaluminumoxane activated iron(II) complexes based on 2,6-bis(imino)pyridine or diphosphine ligands were successfully employed for the polymerization of acrylate monomers in toluene or in THF. The activation process was studied with electrospray ionization mass spectrometry, and a four-coordinated cationic methyl iron(II) complex was identified as one of the products formed by the treatment of 2,6-bis[1-(2,6-diisopropylphenylimino)ethyl]pyridine iron(II) chloride with MAO. The polymerization mechanism was studied in detail by means of kinetic investigations, polymer end-groups analysis and UV-Visible spectroscopy, and compared to the literature data available for related catalytic systems. Even though the intimate polymerization mechanism could not be ascertained, it was demonstrated that coordination of acrylate to the iron center takes place during the propagation step in toluene, whereas termination proceeds via β -hydride transfer to the metal for 2,6-bis(imino)pyridine based catalysts and through transfer to aluminum with diphosphine based catalysts. Furthermore, copolymerization of *tert*-butyl acrylate with 1-hexene was achieved, forming a random copolymer.

Preface

This work has been carried out during the years 2001-2005 at the Laboratory of Inorganic Chemistry, University of Helsinki, Finland.

I would like to express here my deepest gratitude to Professor Markku Leskelä and Docent Timo Repo for giving me the opportunity of accomplishing my PhD studies in their research group, and for the guidance and support I received from them during these four years.

I also would like to thank my colleagues from the Catlab for all the help and support I received inside and outside the department. Especially my labmate Antti, his friend Kirill (and his Sebastopol discussions), Petro, Arto, and my office mates Kristian and Mika whose help was essential during my first steps in Helsinki. A special thank to my friend and colleague Professor Mohamed Lahcini for all the moments we shared from Bordeaux to Helsinki.

I am grateful to Amélie, Yannick, Xixilu, John, Pierre-Louis, Muriel, Patxi (merxi pour les coups de fil du samedi soir) eta Evelyne for being this much supportive despite the years and the 3500 km which have been separating us. I don't forget my grandparents François et Elda (che robate!!!), tonton Alain et tatie Cécile, Delphine, Fred, Juliette, Gilles and co. And a special thank to Holger for bringing me laughs and joy.

I want to thank my friends here in Helsinki: Georges of course, but also Nicolas B. and Saija, Brian, Neil, Raouf, Raphaël and Victoria and all the WRC members. Special thank also to Abigaëlle, Lucie and Inès. I guess it would have been harder without you here in Helsinki. Thank you all of you back there in France (and around): Christophe, Perrin, Polox, Et et El, Edmond, Benito, Tonton Fredo, Xeb et Sab, Anita, Mikel, Franki, Etxe, Cloclo, Cousin Guigui, Cousin Peyo, Pantxo, Pierrot, Didiax, Ricardo, Xabi I., Matthieu A. (ze colloc), Alain et Marie-Christine, Roseau, Sergio la Barbouze, Jon, Charlouze, Fézénial, Canèje, Lilian, Juju L., Sandrine, Lolo H., Nadine, Alan, Jacky et Annie, and all who I forget. Thank you for still being my friends (I hope...) in spite of the years and the distance.

I would like to thank the person who has always been supporting me in all my decisions, who has always been pushing me forward and who has always been trusting in me. Mila esker Aita.

The last paragraph of this long list to the dearest among all, thank you Irma for your support in the hardest moments, and for reminding me that there is a life beside chemistry when it was necessary.

Helsinki, May 2005.

List of Original Publications

This thesis is based on the following original publications, which are referred to in the text according to the Roman numerals I-V.

- I. Castro, P. M.; Lappalainen, K.; Ahlgrén, M.; Leskelä, M.; Repo, T. "Iron-Based Catalysts Bearing Bis(imido)-Pyridine Ligands for the Polymerization of tert-Butyl Acrylate" *J. Polym. Sci. Part A: Polym. Chem.* **2003**, *41*, 1380-1389.
- II. Castro, P. M.; Lankinen, M. P.; Uusitalo, A. M.; Leskelä, M.; Repo, T. "Polymerization of Acrylate Monomers by Iron(II) Complexes Bearing bis(Imido)pyridyl or Phosphine Ligand" *Macromol. Symp.* **2004**, *213*, 199-208.
- III. Castro, P. M.; Lahtinen, P.; Axenov, K.; Viidanoja, J.; Kotiaho, T.; Leskelä, M.; Repo, T. "Activation of 2,6-Bis(imino)pyridine Iron(II) Chloride Complexes with Methylaluminumoxane: an Electrospray Tandem Ionization Mass Spectrometry and UV-Visible Spectroscopy Study" *Organometallics*, article in press.
- IV. Castro, P. M.; Leskelä, M.; Repo, T. "Insight Into the Polymerization of tert-Butyl Acrylate by the MAO Activated 2,6-Bis[1-(isopropylimino)ethyl]pyridine Iron(II) Complex" (*manuscript*).
- V. Castro, P. M.; Lankinen, M. P.; Leskelä, M.; Repo, T. "Polymerisation of Acrylates Catalysed by Methylaluminumoxane Activated Ditertiary Phosphine Complexes of Iron and Cobalt Dichlorides" *Macromol. Chem. Phys.* **2005**, *206*, 1090-1097.

Abbreviations

acac	Acetylacetonate
amu	Atomic Mass Unit
AN	Acrylonitrile
ATRA	Atom Transfer Radical Addition
ATRP	Atom Transfer Radical Polymerization
biPy	2,2'-Bipyridine
CCT	Catalytic Chain Transfer
CID	Collision Induced Dissociation
Cp	Cyclopentadienyl
Cp*	Permethylated cyclopentadienyl
CTA	Chain Transfer Agent
DPPP	1,3-bis(diphenylphosphino)propane
ESI	Electrospray Ionization
Et	Ethyl
GC	Gas Chromatography
GTP	Group Transfer Polymerization
iPr	Isopropyl
IR	Infra-Red spectroscopy
L	Ancillary ligand (general)
LMCT	Ligand to Metal Charge Transfer
M	Any transition or rare-earth metal
MA	Methyl Acrylate
MAO	Methylaluminumoxane
Me	Methyl
MMA	Methyl Methacrylate
M_n	Number average molecular weight
MS	Mass Spectrometry
MWD	Molecular Weight Distribution
Pf	Pentafluorophenyl
Ph	Phenyl
R	Any alkyl group
SHOP	Shell Higher Olefin Process
<i>t</i> BA	<i>tert</i> -Butyl Acrylate
<i>t</i> BMA	<i>tert</i> -Butyl methacrylate
T_g	Glass transition temperature
THF	Tetrahydrofuran
THT	Tetrahydrothiophene
TMA	Trimethyl Aluminum
UV-Vis	UV-Visible spectroscopy

Table of Contents

ABSTRACT	3
PREFACE	4
LIST OF ORIGINAL PUBLICATIONS	5
ABBREVIATIONS	6
TABLE OF CONTENTS	7
1 INTRODUCTION	9
2 SCOPE OF THE THESIS	10
3 BACKGROUND	10
3.1 Homogeneous transition metal catalysts for the polymerization of olefins	10
3.2 Late transition metal complexes as polymerization catalysts	12
3.3 Polymerization of (meth)acrylates with transition metal complexes.....	15
3.4 Copolymerization of acrylates with olefins.....	24
4 EXPERIMENTAL	26
4.1 General	26
4.2 Polymerization	26
4.3 Determination of the kinetic rate orders	26
5 2,6-BIS(IMINO)PYRIDINE IRON (II) COMPLEXES: SYNTHESIS AND CHARACTERIZATION	27

6	ACTIVATION PROCESS: IDENTIFICATION OF THE ACTIVE SPECIES	30
6.1	Literature survey	30
6.2	ESI-MS / UV-Vis investigations.....	31
7	MAO ACTIVATED 2,6-BIS(IMINO)PYRIDINE IRON COMPLEXES FOR THE POLYMERIZATION OF ACRYLATES	37
7.1	Potential mechanisms	37
7.2	Polymerization	39
7.3	Concluding remarks about the polymerization mechanism	49
8	DIPHOSPHINE IRON(II) CHLORIDE COMPLEXES	53
8.1	Polymerization of MA with iron(II) catalysts.....	53
8.2	Nature of the active species	55
9	CONCLUSION	57

1 Introduction

Polymers bearing polar functionalities like poly((meth)acrylate) are readily synthesized via traditional free-radical or ionic chain polymerization. However, precise control over the polymerization behavior and polymer characteristics such as number average molecular weight (M_n) or molecular weight distribution (MWD) is hardly achieved due to the multitude of active species present in the polymerization system, and to uncontrollable chain-breaking reactions such as termination and transfer.^{1,2} Consequently, since the original discovery of “living” polymerization by Szwarc in the mid 1950’s,^{3,4} a great deal of interest has been devoted to the attainment of controlled living radical^{5,6} or anionic^{7,8} polymerizations.

The introduction of zirconocene⁹⁻¹¹ and lanthanocene¹²⁻¹⁵ *single-center* catalysts for the polymerization of (meth)acrylates won a great deal of attention as they provide a uniform reacting center for the living stereospecific synthesis of poly(meth)acrylates with high molecular weight and narrow MWD. However, in spite of these remarkable polymerization abilities, Group 4 and lanthanide based catalysts present some major drawbacks: an arduous synthesis as well as a high Lewis acidity which worsens their sensitivity to the presence of lowly traces of Lewis base or protic impurities. The corollary is that such catalysts require cautious handling in addition to intricate purification processes regarding the solvents, monomers or other reagents. Furthermore, the strictly anionic character of the polymerization precludes the attainment of highly desirable random copolymers with α -olefins,¹⁶ a new generation of polyolefinic materials displaying enhanced properties such as adhesion, toughness or miscibility with other polymers.

In this regard, the advent of late transition metal based olefin polymerization catalysts¹⁷⁻¹⁹ in the mid nineties opened up a new horizon in the field of metal catalyzed homo- and copolymerization of polar monomers, since late transition metals are less oxophilic and are therefore supposed to be more tolerant toward Lewis bases than lanthanides or early transition metals.^{16,18} Indeed, nickel(II) and palladium(II) complexes used in olefin polymerization were reported to tolerate heteroatoms²⁰ and even to incorporate polar monomers into α -olefin polymers.²¹⁻²³ More recently, it was

demonstrated that 2,6-bis(imino)pyridine based iron(II) catalysts homopolymerize various vinylic polar monomers with low conversion in the presence of ethylene.²⁴ It is in this context that we have considered to homopolymerize acrylate monomers with methylaluminoxane (MAO) activated iron(II) chloride complexes bearing bi- or tridentate donor ligands.

2 Scope of the Thesis

At the commencement of this work, it rapidly became obvious that a polymer is formed when MAO, an iron precatalyst and *tert*-butyl acrylate (*t*BA) are mixed together in an appropriate solvent. However, the empirical observation being established, a question started to rise in our minds: “*How does it work?*”

Actually, before the time we started this research, a number of reports describing the homopolymerization of (meth)acrylates promoted by a two-component catalyst consisting of a late transition metal complex and an alkyl aluminum co-catalyst had already been published by diverse research groups, in particular with alkylaluminoxane activated nickel²⁵⁻³² or palladium³³ complexes. Nevertheless, to date, little is known about the nature of the propagating species as well as about the polymerization mechanism, *i.e.* the propagation pathway, the exact role of the co-catalyst, and the happenings at the metal center in the presence of a monomer. The goal of this research was therefore to gain a better insight into the intimate mechanism of the polymerization of acrylate monomers catalyzed by MAO activated 2,6-bis(imino)pyridine and diphosphine iron dichloride complexes.

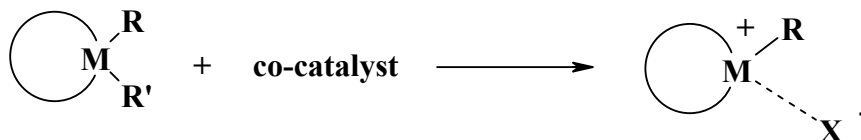
3 Background

3.1 Homogeneous transition metal catalysts for the polymerization of olefins

Soon after the discovery of heterogeneous olefin polymerization catalysis by Ziegler and Natta, the need for homogeneous analogs became obvious in order to study

the details of the polymerization process. In 1957, Natta³⁴ and Breslow³⁵ achieved the polymerization of olefins with a homogeneous two-component system consisting of titanocene Cp_2TiCl_2 in the presence of AlEt_3 or AlEt_2Cl , which anyhow exhibited a lower activity than the TiCl_4 -based heterogeneous system. The discovery of alkylaluminumoxane by Kaminsky at the end of 1970s^{36,37} probably represented one of the most significant advance in organotransition metal chemistry as it marked the beginning of homogeneous catalysis. The comprehension of the different steps of the Ziegler-Natta polymerization and of various other homogeneous metal-based catalysis processes profited from the subsequent rapid development of novel well-defined single-center polymerization catalysts.

Generally speaking, it is agreed that the active species in transition metal catalyzed olefin polymerization is a coordinatively unsaturated cationic alkyl complex of the form $[\text{L}_n\text{MR}]^+$ (L = stabilizing ligand which remains bound to the metal center over the course of the catalytic reaction, M = transition metal or rare-earth metal, R = initiating group or polymer chain). This species is generated by the reaction of a transition metal complex (halide, alkoxide, alkyl or aryl) with a main group organometallic compound (generally an organoaluminum or organoboron) referred to as the co-catalyst (Scheme 1).



Scheme 1. Formation of the catalytically active species. R = alkyl or aryl, R' = halide, alkoxide, alkyl or aryl, X⁻ = co-catalyst based counter-anion.

The main co-catalyst used in the activation of homogeneous transition metal polymerization catalysts is MAO, which is produced via the controlled hydrolysis of trimethylaluminum (TMA) by, for instance, $\text{Al}_2(\text{SO}_4)_3$ hydrates.³⁷ It is generally presented as an oligomeric compound consisting of 5 to 20 $-\text{[Al(Me)-O]}-$ subunits. However, its exact composition has still not been clarified, and different structures have been proposed, ranging from one-dimensional linear or cyclic oligomers to three-dimensional clusters. Structural elucidation is challenging because of the multiple

equilibria present in the MAO solution, and due to the presence of residual free or MAO bonded TMA.³⁸ Furthermore, as the co-catalyst, methylaluminoxane (MAO) is not only expected to form the polymerization active species by reacting with the metal complex, but also to scavenge impurities susceptible to hampering the polymerization.³⁹

3.2 Late transition metal complexes as polymerization catalysts

At the beginning of the 1950s, while the chain growth of ethylene on aluminum alkyls (the “Aufbaureaktion”) constituted state-of-the-art polymer chemistry,⁴⁰ Karl Ziegler recognized that the failure of one of many “Aufbaureaktionen” was due to the presence of small amounts of nickel salts in the reactor which were acting as a co-catalyst, producing 1-butene instead of the expected polyethylene. The discovery of this “Nickel-Effect” led him and his collaborators to look for other transition metals providing a similar effect, which ended up in the breakthrough of zirconium and titanium catalysts capable of polymerizing ethylene to high molecular weight polyethylene, the “Ziegler Catalysts.”⁴¹ This brief but decisive appearance of nickel in the realm of polymerization (in fact, oligomerization) catalysis might however represent one of the first reported late transition metal catalyzed oligomerization of olefinic monomers.

At the time of this discovery, little was known about transition metal alkyls, apart from the platinum alkyls, principally because of their high instability.⁴² What was known of the polymerization process was mainly derived from speculations about olefin π -coordination to a transition metal alkyl and subsequent insertion into the metal-carbon bond.^{43,44} In parallel to the work of Natta and Breslow on titanocenes (paragraph 3.1), the search for model complexes matching the catalyst structure during the olefin coordination and insertion steps postulated in the Cossee’s mechanism⁴³ led, in the mid 1960s, the group of Yamamoto to the isolation of the diethyl complexes of nickel and iron bearing a stabilizing 2,2’-bipyridine ligand ($\text{NiEt}_2(\text{biPy})$ and $\text{FeEt}_2(\text{biPy})_2$).⁴⁵⁻⁴⁸ These complexes were successfully employed for the polymerization of various vinylic monomers such as acrylonitrile (AN), methyl methacrylate (MMA) or methyl acrylate.⁴⁹⁻⁵² The work accomplished over almost a decade resulted in evidencing some of the

elementary processes involved in metal catalyzed polymerization of olefins – for instance π -coordination, insertion or β -hydride elimination – and governing organotransition metal chemistry like reductive elimination.^{53,54}

In spite of these remarkable findings, the use of late transition metal complexes as polymerization catalysts remained trivial. Functionalized monomers were already polymerized by radical or ionic initiators, and the tremendous developments of the then renamed “Ziegler-Natta” catalysts – worth a joint Noble price awarded to Professors Karl Ziegler and Giulio Natta in 1963 – totally obscured the research carried out at the academic level concerning late transition metal polymerization catalysts. Moreover, ethylene or α -olefins polymerization was hardly achieved with late metal catalysts as a consequence of favored β -hydride elimination and/or reductive elimination of the growing polymer chain leading to deactivated metal complexes.¹⁸ In fact, owing to the competing β -hydride elimination, the ability of nickel catalysts to selectively oligomerize ethylene was turned into an industrial opportunity at the end of the 1960s under the appellation the Shell Higher Olefin Process (SHOP), providing linear α -olefins (C₆-C₂₀).^{18,55}

The research devoted to Group 4 metal complexes was further accelerated after the advent of MAO and efficient metallocene polymerization catalysts,³⁷ narrowing the possibilities of new discoveries and patent applications. The consequence was a growing interest at both the academic and industrial level in new polymerization catalysts which pushed researchers to investigate the potential of other transition metals in the polymerization of ethylene and of higher α -olefins.^{17,19} The real breakthrough for late transition metal complexes in the area of polymerization catalysis came in the mid 1990s with the discovery by Brookhart and his coworkers that cationic square planar α -diimine nickel and palladium catalysts were capable of polymerizing ethylene or higher α -olefins with high activity, producing polymers whose structures vary from highly branched amorphous to linear semi-crystalline material depending on the ligand and on the reaction conditions.⁵⁶ Living polymerization of α -olefins and block copolymerization were also achieved,^{57,58} while functionalized polyethylene ranging from random ethylene/acrylate copolymer^{21,22,59} to telechelic polyethylene⁵⁸ could be prepared by using an appropriate palladium precursor and/or by proper adjunction of an acrylate feed to the polymerization

reaction. Following this pioneering work, and with the desire to explore untilled parts, from a polymerization catalysis viewpoint, of the Periodic Table, new catalyst precursors based on Fe, Ru, Co, Rh or Cu were designed and successfully utilized to polymerize olefins.¹⁷⁻¹⁹

2,6-Bis(imino)pyridine Iron(II) Chloride Complexes

In the quest for novel late transition metal complexes combining straightforward complex synthesis, low cost and ready availability of the metal to high olefin polymerization activity, Brookhart *et al.*⁶⁰ and Gibson *et al.*⁶¹ described almost simultaneously the use of 2,6-bis(imino)pyridine iron(II) complexes as ethylene polymerization catalysts after their activation with MAO. The catalysts exhibit exceptionally high activities, equivalent to or even higher than those observed with metallocene catalysts under similar polymerization conditions, producing strictly linear high molecular weight polyethylene.

The key feature of the polymerization resides in the steric bulk provided by the *ortho* substituents on the imine aryl groups. According to crystallographic studies, the aryl groups in the dichloro complexes are nearly perpendicular to the plane formed by the bis(imino)pyridil ligand and the iron center, positioning the *ortho* substituents above and below the plane, thus blocking the axial positions (Figure 1).⁶⁰⁻⁶² Experimentally, it was demonstrated that increasing the size of these *ortho* substituents (methyl *vs.* isopropyl) results in an increased degree of polymerization, whereas complexes with only one *ortho* substituent on each aryl group produce oligomers with unsaturated end groups, the sign of a dominant β -hydride chain transfer process.⁶³ It was proposed that the steric protection around the metal center retards β -hydride transfer, thus favoring the chain growth.⁶⁰⁻⁶² This was later confirmed by theoretical studies.^{64,65} In addition to β -hydride transfer, chain transfer to aluminum generates lower molecular weight fractions, inducing bimodal molecular weight distributions.⁶²

The isospecific polymerization of propylene has also been investigated, and proceeds with regioregularity via a 2,1-insertion mechanism. However, lower activity and lower molecular weights were obtained compared to ethylene polymerization.⁶⁶

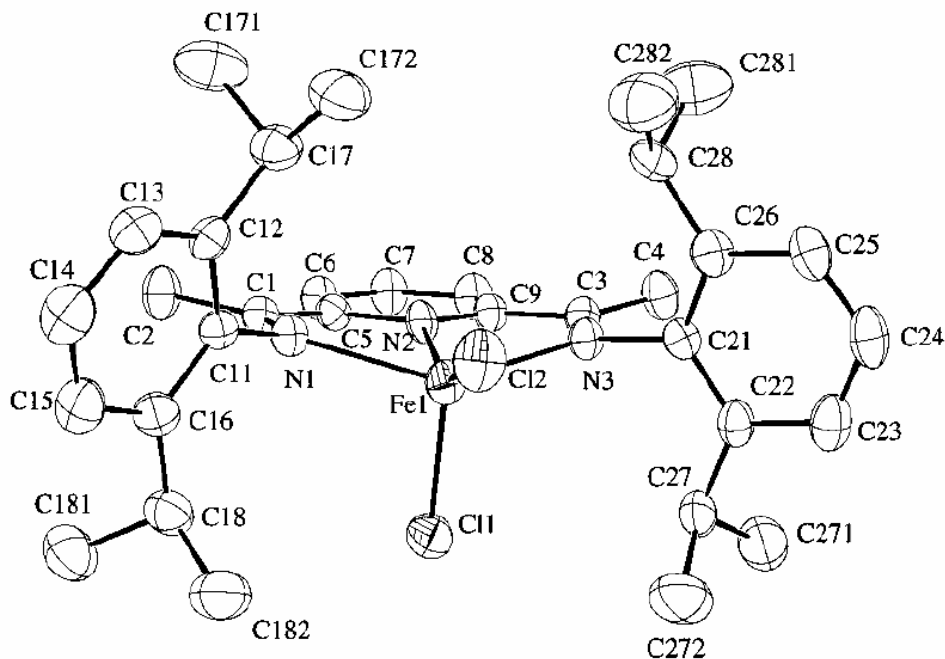


Figure 1. Molecular structure of 2,6-bis[1-(2,6-diisopropylphenylimino)ethyl]pyridine iron(II) chloride (**1**).⁶⁰

3.3 Polymerization of (meth)acrylates with transition metal complexes

In the following, the transition metal-mediated polymerization of (meth)acrylate monomers is reviewed. This part is not meant to be comprehensive but focuses on referencing the diverse polymerization mechanisms reported in the literature which can be related to the present study.

3.3.1 Lanthanides and early transition metal metallocenes: pseudo-anionic polymerization

The cornerstone of metal-mediated polymerization of (meth)acrylate was laid at the beginning of the 1990s when two groups independently reported the living syndiospecific polymerization of methyl methacrylate with d^0/f^n metallocene catalysts. Yasuda *et al.* employed a neutral single-component lanthanide based catalyst ($[\text{Cp}^*_2\text{SmH}]_2$) to produce highly syndiotactic ($[rr] = 95\%$ at -95°C) poly(MMA) in high yield, with high molecular

weight ($> 10^6$ g/mol) and narrow MWD (< 1.05).¹² The polymerization mechanism could be established thanks to the isolation of the 1:2 adduct of $[\text{Cp}^*_2\text{SmH}]_2$ with MMA. The single-crystal X-Ray analysis of this $\text{Cp}^*_2\text{Sm}(\text{MMA})_2\text{H}$ complex indicated that one of the MMA connects to the metal in an enolate form while the second is coordinated to the Sm center through its carbonyl C=O group, forming an eight-membered cyclic intermediate (Figure 2). On this basis, the initiation was proposed to occur via the 1,4-conjugated addition of the metal-hydride to the first MMA double bond, forming a transient $\text{Cp}^*_2\text{SmOC}(\text{OCH}_3)=\text{C}(\text{CH}_3)_2$ which subsequently reacts with the second MMA to form the cyclic $\text{Cp}^*_2\text{Sm}(\text{MMA})_2\text{H}$ complex. Propagation proceeds in a similar fashion in the presence of additional monomers (Scheme 2), analogously to the group-transfer mechanism reported for organosilicon initiated polymerization of α,β -unsaturated esters.⁶⁷

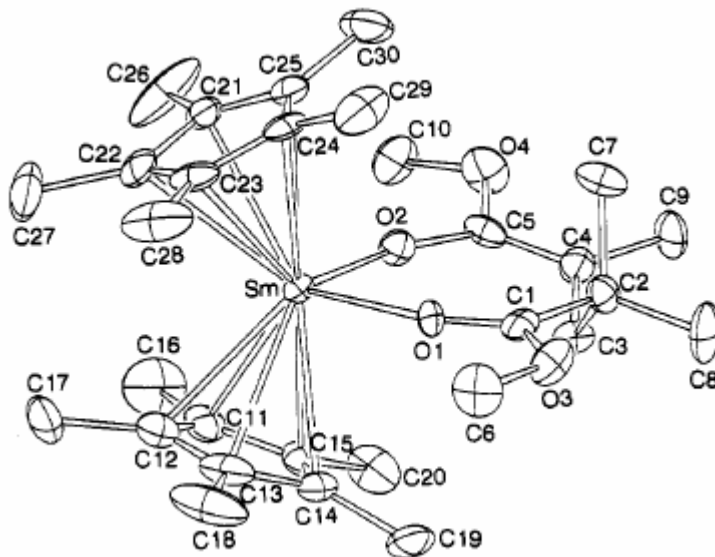
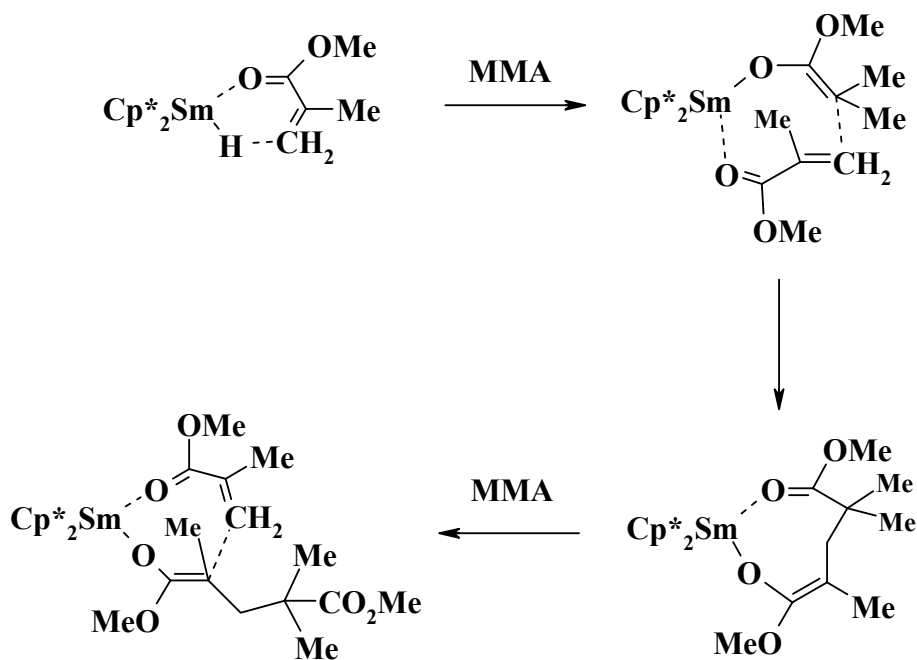
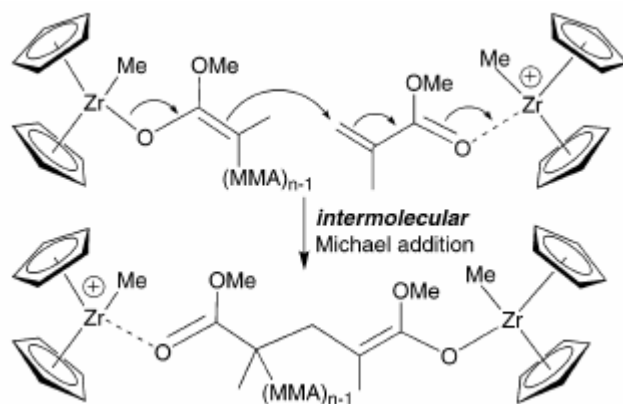


Figure 2. ORTEP view of $\text{Cp}^*_2\text{Sm}(\text{MMA})_2\text{H}$.¹²



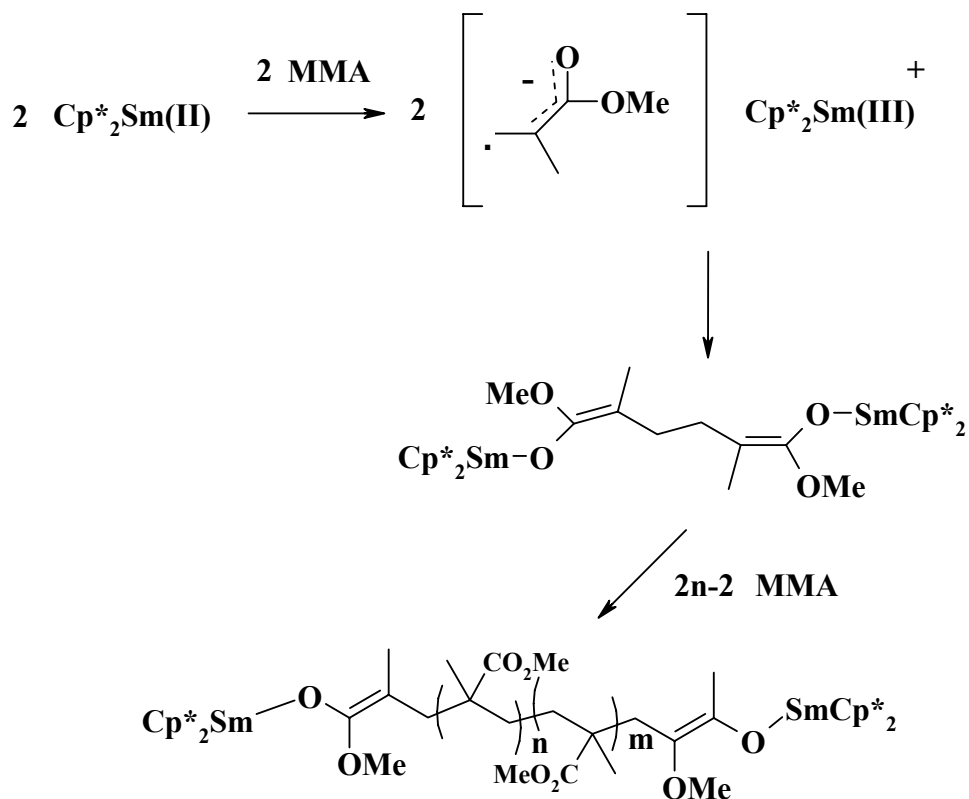
Scheme 2. Initiation mechanism for the polymerization of MMA with Cp^*_2SmH .¹³

The two-component system consisting of a cationic zirconocenium complex $\text{Cp}_2\text{ZrMe}(\text{THF})^+\text{BPh}_4^-$ and a neutral zirconocene Cp_2ZrMe_2 described by Collins *et al.* also achieved controlled polymerization of MMA, but with a lower amount of syndiotactic dyads (80%) and higher MWD (1.2–1.4).⁹ The initiation was later demonstrated to proceed via intramolecular 1,4-addition of the Me group from the cationic complex to an O-coordinated MMA, producing a transient cationic enolate complex which is further transformed to a neutral $\text{Cp}_2(\text{Me})\text{ZrOC}(\text{OCH}_3)=\text{C}(\text{Et})(\text{Me})$ by reaction with Cp_2ZrMe_2 .^{68,69} The propagation occurs by intermolecular Michael addition of the zirconocene enolate to a MMA unit activated by the cationic zirconocene, consistent with a bimetallic version of the mechanism proposed by Yasuda (Scheme 3). The use of a preformed neutral enolate initiator with the cationic zirconocene ensued faster initiation rates and narrower MWDs.^{68,69}



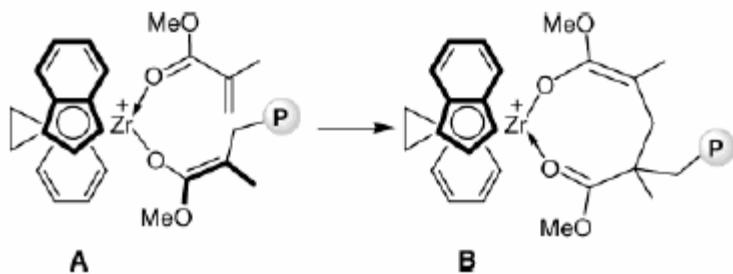
Scheme 3. Bimetallic group transfer polymerization (GTP) mechanism.⁷⁷

Further developments in d^0/f^n metallocene-mediated polymerization of (meth)acrylate were not only motivated by the scientific challenge consisting of the antinomic combination of highly electrodeficient transition metal complexes and polar monomers, but also by the high activities and degree of control attained. In lanthanide based initiators, it was found that the activity is directly dependent on the metal and decreases with an increased ionic radius ($\text{Sm} > \text{Yb} > \text{Lu}$).¹³ Different types of initiators were also employed apart from the dimeric $[\text{Cp}^* \text{M}(\mu\text{-Me})_2]_2$: single-component monomeric $\text{Cp}^* \text{M-Me}(\text{THF})$ ($\text{M} = \text{Sm}, \text{Yb}, \text{Lu}$) or bimetallic $\text{Cp}^* \text{M}(\mu\text{-Me})_2\text{AlMe}_2$ ($\text{M} = \text{Yb}, \text{Lu}$), all showing similar initiation properties and yielding MMA polymers with comparable characteristics.¹³ Soon after, chiral C_1 ligands were introduced and the isospecific polymerization of MMA was performed, although it was not clear if the stereocontrol was due to chain-end or enantiomorphic site control.⁷⁰ A *mm* diad content of 94% was obtained at -35°C , but with high polydispersity ($\text{MWD} = 7.9$). Stereospecificity is not limited to the use of lanthanocenes as Arnold *et al.* employed the non-metallocene single-component bis(pyrrolylaldiminato) $\text{Sm-CH}_2(\text{SiMe}_3)$ complex to achieve the highly isospecific polymerization of MMA at room temperature ($mm = 95\%$), with relatively narrow MWD (< 2).⁷¹ Organolanthanide complexes (Sm and Yb) in the +2 oxidation state were also found to produce poly(MMA) in a controlled manner.¹³ Initiation takes place via the formation of a bis-initiator: a radical anion is formed via a one-electron transfer from one initiator to the first MMA. Subsequent coupling with a second MMA gives a bimetallic bis-enolate complex which initiates the polymerization (Scheme 4).^{14,72}



Scheme 4. Initiation mechanism with a Sm(II) complex.¹⁴

Regarding Group 4 complexes, single-component initiators consisting of a dimethyl zirconocene and a borate activator were successfully employed to polymerize MMA, in the presence^{10,11} or in the absence⁷³ of an added Lewis acid (ZnEt_2). One of the most significant improvement of the catalytic system is undeniably the introduction of chiral *ansa*-zirconocenes^{10,11,68,73,74} which permitted the synthesis of isotactic poly(MMA) via enantiomorphic site control. Investigations of the propagation mechanism leading to isospecificity revealed that with single-component initiators such as $[\text{Me}_2\text{CCp}(\text{Ind})\text{ZrMe}(\text{THF})]^+[\text{BPh}_4]^-$, the polymerization proceeds via a monometallic mechanism similar to the Yasuda mechanism, and that isospecificity is induced by epimerization of the active-site after each propagating step.⁷⁵ This was further confirmed by the work of Chen and his coworkers who isolated a model compound of the *rac*- $\text{C}_2\text{H}_4(\text{Ind})_2\text{Zr}^+(\text{THF})[\text{OC}(\text{OiPr})=\text{CMe}_2][\text{MeB}(\text{C}_6\text{F}_5)_3]^-$ catalyst resting state similar to the Yasuda's $\text{Cp}^*_2\text{Sm}(\text{MMA})_2\text{H}$ complex (Scheme 5).^{76,77}

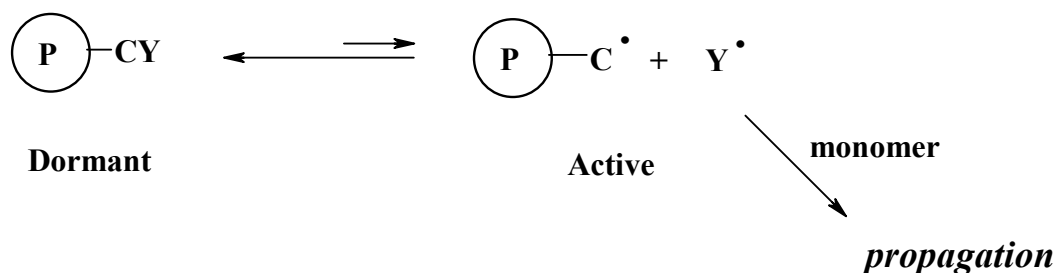


Scheme 5. Propagating species (A) and resting species (B) in the *rac*-C₂H₄(Ind)₂Zr⁺(THF)[OC(OiPr)=CMe₂][MeB(C₆F₅)₃]⁻ catalyzed polymerization of MMA.⁷⁶

3.3.2 Late transition metal-mediated polymerization of polar monomers: from radical to coordination/insertion

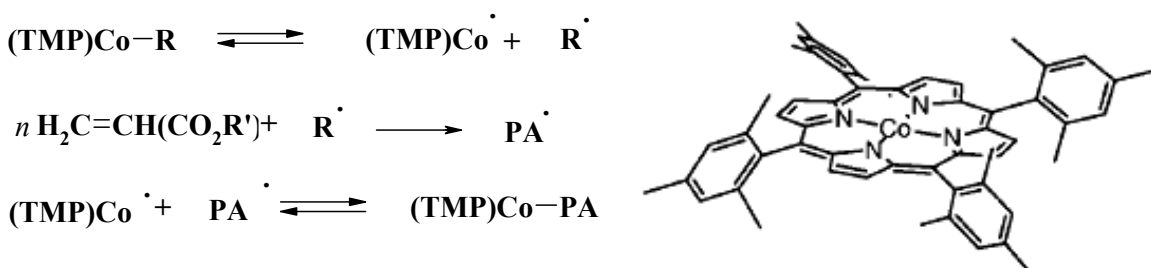
Radical polymerization

Several approaches have been recently introduced in order to obtain chain-growth control in radical polymerization. Mainly, living radical polymerization is achieved by controlling the radical concentration through its equilibration with a dormant species. By maintaining a low concentration of propagating radicals, chain termination reactions such as coupling or disproportionation are avoided (Scheme 6).⁷⁸ The most prominent and probably the most studied metal-mediated living radical polymerization system is atom-transfer radical polymerization (ATRP).^{79,80}



Scheme 6. Living radical polymerization.

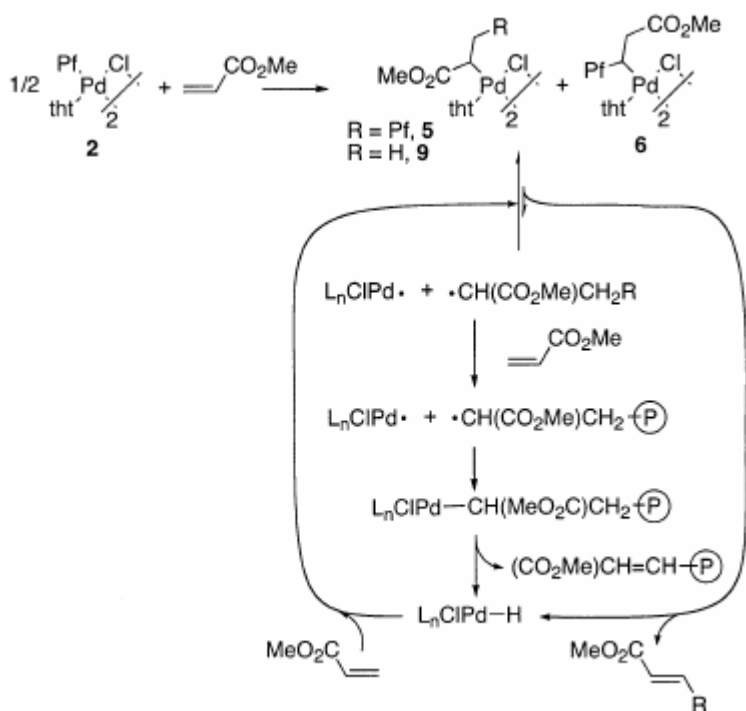
Transition metal-mediated controlled living radical polymerization can be obtained from organometallic complexes. For instance, cobaloximes and related cobalt complexes have been widely investigated since the mid 1970s as chain transfer agents (CTA) for the catalytic chain transfer (CCT) to monomer in free-radical polymerization.^{81,82} More recently, the homo- and block copolymerization of acrylates initiated with organocobalt porphyrins was reported by Wayland and coworkers.^{83,84} At a moderate temperature (60°C), the thermally induced cobalt-carbon bond homolysis of tetramesityl porphyrinato cobalt(III)-organo complexes ((TMP)Co-R) provides organic radicals R[•] able to initiate the polymerization by reacting with an acrylate monomer, and a stable metal-centered radical (TMP)Co(II)[•] acting as a capping agent (Scheme 7). The propagating chain recombines reversibly with (TMP)Co(II)[•], ensuring a low concentration of radicals throughout the polymerization process. The living nature of the polymerization was ascertained according to the linear increase of M_n with monomer conversion, the relatively low MWD (1.1 – 1.2) and the formation of block copolymers. The presence of (TMP)Co-polymer species in the polymerization solution was evidenced by ¹H NMR, and the quasi-absence of β-H transfer to metal was explained by the steric hindrance of the ligand.



Scheme 7. Mechanism of the cobalt-mediated radical polymerization of MA (left),⁷⁸ and structure of (TMP)Co (right).⁸²

Still, late transition metal-mediated radical polymerization through the homolysis of a metal-carbon bond is not the prerogative of cobalt(III) complexes. For instance, Novak *et al.* reported the use of neutral palladium methyl complexes bearing pyrrole-imine ligands as efficient single-component initiators for the homopolymerization of MA

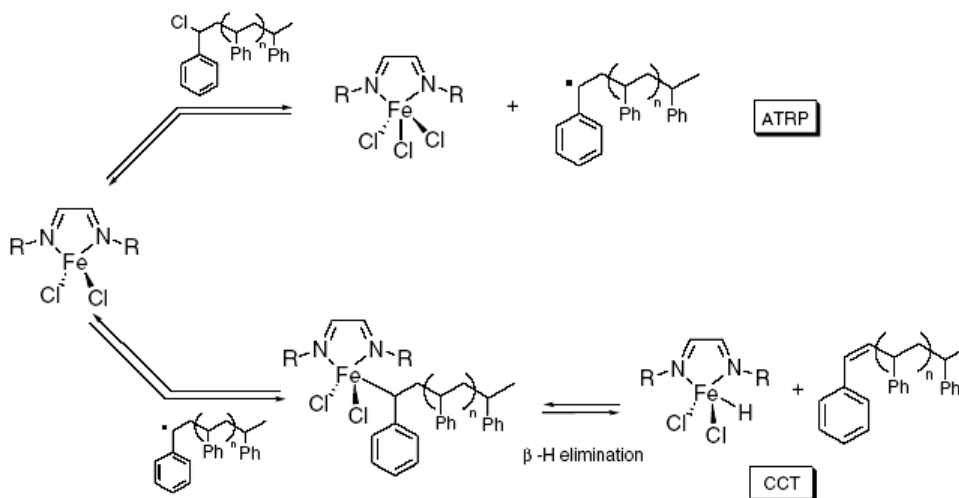
and its copolymerization with norbornene or 1-hexene.⁸⁵ Isolated enolate analog complexes, potential reaction intermediates in the case of a coordination/insertion or pseudo-anionic mechanism, were proved inactive in initiating the polymerization. Furthermore, polymerization was halted by an appropriate radical scavenger, galvinoxyl. On this basis, a radical mechanism similar to organocobalt initiated polymerization was proposed, as the initiation step was believed to take place via homolytic cleavage of the Pd-Me bond. Following this study, neutral palladium and/or nickel complexes bearing acetylide⁸⁶ or pentafluorophenyl (Pf)^{87,88} initiating groups were also found to be effective initiators for the radical polymerization of (meth)acrylates. In addition, in the case of Pf substituted palladium initiators, initiation was demonstrated to occur after insertion of the acrylate into the Pd-aryl bond, and subsequent homolysis of the metal-carbon bond. Chain transfer was provided via β -hydride elimination, generating a Pd-H species able to re-initiate the polymerization after monomer insertion (Scheme 8). Copolymerization with 1-alkenes was also achieved.^{87,88}



Scheme 8. Mechanism for the $\text{Pd}_2(\mu\text{-Cl})_2\text{Pf}_2\text{tht}_2$ mediated radical polymerization of MA (tht = tetrahydrothiophene).⁸⁸

Regarding iron complexes, five-coordinated alkyliron(III) porphyrin complexes are known to be relatively unstable and to reversibly undergo iron-carbon bond homolysis, even at ambient temperature.⁸⁹⁻⁹¹ Consequently, *n*-butyl iron(III) tetraphenylporphyrin and *n*-butyl iron(III) tetrakis-(pentafluorophenyl)porphyrin were evaluated for the polymerization of styrene, MMA or 1-pentene.⁹² However, the low energy of the iron-carbon bond, weaker than in cobalt analogs, does not provide a sufficient capping effect from iron(II) centered radicals, and the resulting high concentration of free *n*-butyl radicals rapidly terminates the polymerization by recombination with the growing radical, yielding oligomers with a low conversion.

An intriguing catalytic system based on iron(II) chlorides bearing a bi- or tridentate nitrogen ligand polymerizing styrene and MMA in the presence of a haloester initiator was described by Gibson and coworkers.⁹³⁻⁹⁵ Complexes possessing an N-alkyl substituent proved to be efficient ATRP catalysts, according to the presence of a halogen end-group in the polymer, while N-aryl substituted analogs did not provide controlled polymerization, and unsaturated end-groups were recovered. It was proposed that ATRP was operating in the former case, while CCT was the main event in the latter case (Scheme 9).



Scheme 9. Competing ATRP and CCT polymerization mechanisms.⁹⁵

MAO activated complexes for the polymerization of (meth)acrylates

MAO activated late-transition metal complexes have been reported for more than a decade to polymerize methacrylate monomers. The use of di-acetylacetonate (acac) complexes of Ni in conjunction with MAO provided moderate conversions, relatively narrow MWD (1.25 – 4.61) and high M_n (50 – 90 kg/mol) in the polymerization of MMA,^{25,26} and high conversions (close to 100%), low MWD (1.4 – 2.1) and high M_n (140 – 210 kg/mol) with *tert*-butyl methacrylate (*t*BMA).⁹⁶ Later, diverse nickel catalysts bearing ligands like salicylaldiminate,^{30,31} β -ketoamine N,O-chelate,³² dicyclopentadienyl^{27,28} or bis-phosphine²⁷ were introduced. Kinetic investigations of the Ni(acac)₂/MAO catalyzed MMA polymerization revealed a first order dependence of the propagation rate on monomer concentration, and a 0.6 reaction order on the catalyst Ni(acac)₂/MAO concentration. On this basis, the polymerization mechanism was proposed to occur via coordination of the monomer to the nickel center and subsequent insertion into a nickel-carbon bond.²⁹ A similar mechanism was claimed for salicylaldiminate based catalysts.³⁰

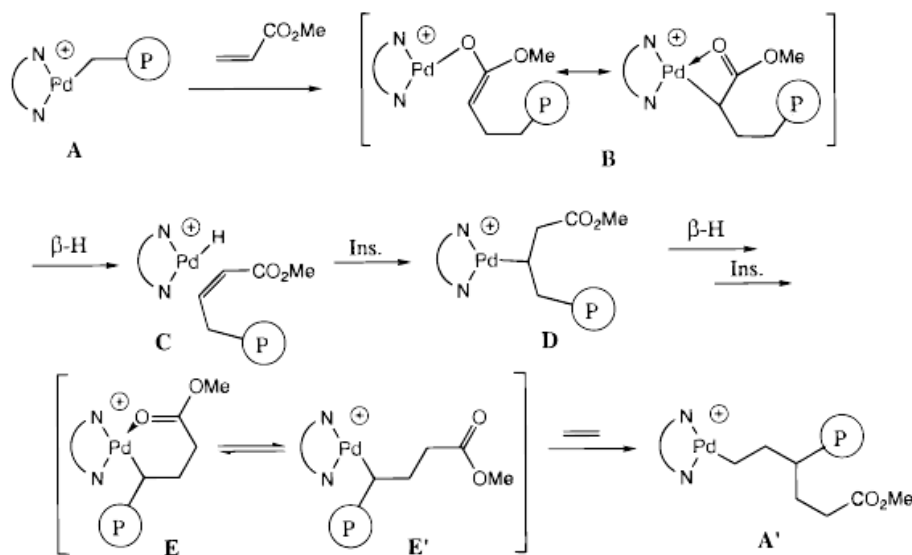
Apart from nickel, diverse MAO activated late-transition metal based catalysts were employed in the polymerization of (meth)acrylate monomers: Fe,^{97,98} Co,⁹⁷ Pd³³ or Cu.⁹⁹ Nevertheless, a common feature between those diverse studies is that no clear mechanistic indication could be obtained, most probably because of the presence of an excess of MAO in the polymerization media.

3.4 Copolymerization of acrylates with olefins

If copolymerizing polar monomers with ethylene or higher α -olefins under mild conditions was until recently a challenging issue,¹⁶ it is nowadays merely achieved via radical-mediated polymerization by metal complexes,^{85,87,100} nitroxide¹⁰¹ or reversible addition-fragmentation chain transfer (RAFT).¹⁰² Regarding late transition metal catalyzed copolymerization, as stated earlier (chapter 3.2) the tolerance of cationic palladium α -diimine catalysts towards functional-groups permits the copolymerization of ethylene with functionalized olefins such as acrylates.²¹ Thanks to detailed low-temperature NMR mechanistic investigations, polymerization intermediates were

spectroscopically observed and identified.^{21,22} According to Brookhart *et al.*, acrylate insertion proceeds in a 2,1-mode, yielding a C-bound enolate intermediate in which the carbonyl oxygen binds to the palladium. This transient intermediate rearranges into a more stable six-membered chelate structure, defined as the catalyst resting-state from which further ethylene insertion will take place. This isomerization from four- to six-membered chelate explains the isolation of the ester functionality at a chain/branch end (Scheme 10). Later, Drent *et al.* reported the random copolymerization of various acrylates with ethylene, producing linear polymer in which acrylate units are incorporated into the polyethylene backbone via a coordination/insertion mechanism.⁵⁹ MAO activated nickel complexes were also proved to be efficient catalysts for the copolymerization of ethylene and MMA, leading to a high incorporation of methacrylate units (up to 81%),¹⁰³ whereas MAO activated 2,6-bis(imino)pyridine iron(II) complexes were found to be unsuccessful in achieving the copolymerization. Instead, only blends of homopolymers were recovered.²⁴

On the other hand, early transition metal^{104,105} and lanthanide¹⁰⁶ catalysts can copolymerize α -olefins and (meth)acrylate monomers, but only in an A-B block fashion. It has been pointed out that the copolymer is always ethylene-co-(meth)acrylate since each block is formed via a distinct mechanism in an irreversible manner.^{16,107}



Scheme 10. Mechanism of the ethylene/acrylate copolymerization with cationic palladium catalyst.¹⁶

4 Experimental

4.1 General

All the solvents were dried over sodium and purified by distillation before use. MAO was used as a 10% or 30% solution in toluene. Other reagents used in the syntheses of the complexes and in the polymerizations were purchased from commercial sources with high purity grade, and used without further purification. All the manipulation, syntheses and polymerizations were performed under an argon atmosphere at room temperature in Schlenk glassware with standard Schlenk techniques, or in a glove-box.

Samples for UV-Vis measurement were withdrawn from the catalyst solution and transferred under an argon atmosphere to a gas-tight rectangular quartz cuvette (10 mm path length) fitted with a silicon septum.^{III,IV}

4.2 Polymerization

Polymerizations of acrylate monomers were carried out using toluene^{I,IV,V} or THF^{II} as the solvent. The reagents were introduced in the following order: iron complex, solvent, MAO and monomer. No induction time was observed before the addition of the monomer.^I Monomer conversions were determined either gravimetrically^{I,V} or by gas chromatography (GC) with *n*-decane as an internal standard.^{II,IV}

When *t*BA was copolymerized with 1-hexene,^{IV} both monomers were introduced at the same time into the toluene solution of 4/MAO ([Fe] = 63 $\mu\text{mol/L}$, MAO/Fe = 250, total volume = 30 mL). Conversion was determined by GC relative to *n*-decane. The relative composition of the copolymers could not be ascertained due to signal overlapping in ¹H NMR.

4.3 Determination of the kinetic rate orders

According to the components of the polymerization system, the polymerization rate R_p can be expressed by the kinetic equation (1)

$$R_p = k_{app}[Fe]^a[MAO]^b[tBA]^c \quad (1)$$

Kinetic orders a , b and c were determined according to the method of initial rates.¹⁰⁸ The concentration of one component Y of the polymerization system (*i.e.* metal complex, co-catalyst or monomer) was varied in successive experiments while the concentrations of the two others were kept constant, so that R_p is expressed according to this sole component (2):

$$R_p = k'_{app}[Y]^X \quad (2)$$

providing in each case a numerical value of R_p at a given concentration (X = rate order relative to Y concentration). The slope of the logarithmic variation of R_p vs. $[Y]$ represents the rate order with respect to Y according to (3):

$$\text{Log } R_p = \text{Log } k'_{app} + X \text{Log } [C] \quad (3)$$

5 2,6-Bis(imino)pyridine Iron (II) Complexes: Synthesis and Characterization

Unlike lanthanide or early transition metal complexes, which are often intricate to synthesize and require cautious handling because of their inherent sensitivity to air and moisture, iron(II) complexes are rather stable and easily accessible. Two different types of iron(II) precatalysts have been used in the first part of this study concerning 2,6-bis(imino)pyridine ligands: four literature known complexes bearing aromatic iminyl substituents (**1**, **2**,⁶⁰⁻⁶⁶ **3**, and **6**¹⁰⁹), and two new complexes bearing aliphatic substituents at the imino position (**4** and **5**)^I (Chart 1).

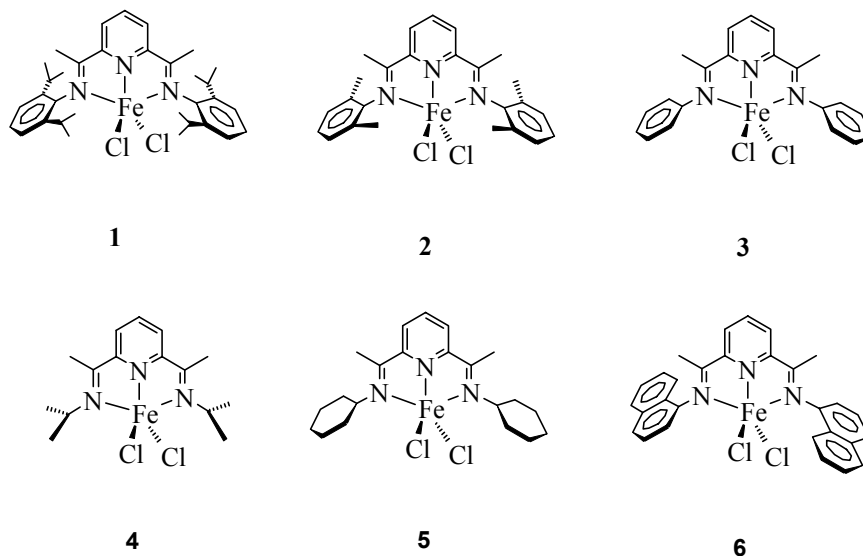
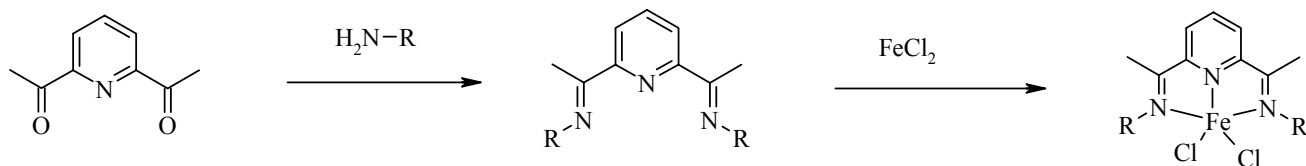


Chart 1. 2,6-Bis(imino)pyridine iron(II) chloride complexes **1-6**.¹

The ligand syntheses were carried out through a classical imine condensation reaction between 2,6-diacetylpyridine and a primary amine (Scheme 11). Ligands **4'** and **5'** (from complexes **4** and **5**) synthesis was carried out in ethanol in the presence of a small amount of Na₂SO₄ (drying agent), at room temperature (**4'**) or in refluxing solvent (**5'**) and monitored with infra-red spectroscopy (IR) by following the disappearance of the carbonyl band (1700 cm⁻¹) of the 2,6-diacetylpyridine and the appearance of the iminyl band (1630 cm⁻¹) characteristic of the iminopyridine. Complexes **1-6** were synthesized by addition of FeCl₂ to a THF solution of the corresponding 2,6-bis(imino)pyridyl ligand at room temperature. The complexes were characterized by IR, mass spectroscopy and elementary analysis. In addition, **4** was subjected to single-crystal X-ray diffraction study (Figure 3). Crystals of **4** suitable for X-ray investigations were obtained from a solution of **4** in CH₂Cl₂ in a saturated pentane atmosphere, which produced short blue needles.



R = 2,6-bis(isopropyl)phenyl (**1**), 2,6-bis(methyl)phenyl (**2**), phenyl (**3**), isopropyl (**4**), cyclohexyl (**5**) or naphthyl (**6**)

Scheme 11. Synthesis of complexes **1-6**.¹

In the solid-state, the iron center is five-coordinated and **4** possess approximately a C_s symmetry about a plane defined by the iron center, the two chlorine atoms and the pyridine nitrogen. Differing from similar complexes bearing 2,6-substituted aryl groups at the imino position like **1** and **2** for which a distorted square pyramidal geometry is reported,^{60,61} the geometry at the iron center in **4** can probably be best described as pseudo-trigonal bipyramidal. The Fe- N(1) (pyridyl) distance is only slightly shorter (2.068(2) Å) than reported for **1** (2.088(4) Å), while the Fe-N (imidos) distances are in good agreement with earlier measurements (Fe-N(3) = 2.237(2) Å, Fe-N(2) = 2.246(2) Å and Fe-N = 2.238(4) Å, 2.250(4) Å, respectively). Also the difference in imido substituents in **1** (aryl) and **4** (isopropyl) is not clearly reflected in the corresponding C=N distances. The N(imido)=C distances in **4** (N(2)=C(6) = 1.293(4) Å and N(3)=C(11) = 1.280(4) Å) are in good accordance with the ones found in **1** (1.285(6) Å and 1.280 (6) Å). The opening of N(2)-Fe-N(3) angle (149.1°) in complex **4** indicates that the iron(II) cation is located deeper in the ligand cavity than in complex **1** (140.1°). The chlorine atoms are above and below the coordination plane of the ligand with unequal distances (Fe-Cl(1) = 2.3466(8) Å and Fe-Cl(2) = 2.2762 (8) Å). Also the Cl-Fe-Cl angle of **4** is wider than observed for **1** (132.00(3)° and 117.5(1)°, respectively).

2,6-Bis(imino)pyridine iron(II) chloride complexes are high-spin paramagnetic species, affording magnetic moments between 5.0 and 5.5 μ_B consistent with four unpaired electrons and a quintet ground state, leading to broad paramagnetically shifted NMR signals.⁶²

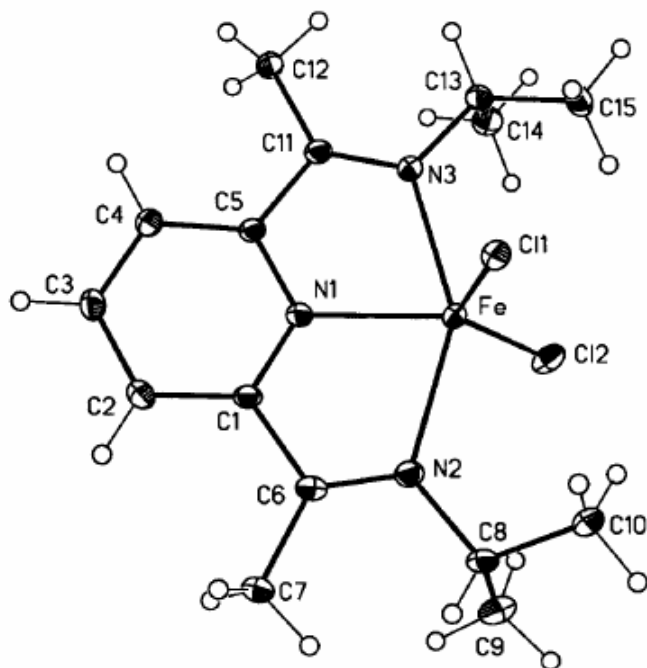


Figure 3. Solid state structure of 4.¹

6 Activation Process: Identification of the Active Species

6.1 Literature survey

The catalytically active species formed by the treatment of 2,6-bis(imino)pyridine iron(II) chloride complexes with MAO is generally proposed to be a highly reactive monomethylated iron(II) cation $[\text{LFe-Me}]^+$ (L = 2,6-bis(imino)pyridine ligand) bearing a weakly coordinating counter-anion $[\text{Me-MAO}]^-$ (paragraph 3.1).^{62,65,66,110,111} Both monochloride and monoalkyl cationic species are expected to be present in the solution, their relative concentration depending on the MAO/Fe ratio. Typically, the use of 100 equivalents of MAO relative to the amount of iron precursor is sufficient to achieve the polymerization of α -olefins.^{62,66}

Coordinationally unsaturated monoalkyl metal cations are likely to interact with other molecules present in the solution, *i.e.* solvent or co-catalyst. Indeed, referring to early transition metal catalysts, bimetallic metallocene species of the type $[\text{Cp}_2\text{M}(\mu-$

$(\text{Me})_2\text{AlMe}_2]^+[\text{Me-MAO}]^-$ (M = Group 4 metal) have been identified, and are believed to be the dormant state of the catalytically active $[\text{Cp}_2\text{M-Me}]^+[\text{Me-MAO}]^-$ ion pair, the position of the equilibrium between these two species governing the catalyst activity.^{38,112-114} Correspondingly, the formation of hetero-binuclear Fe-Al complexes of the type $[\text{LFe(II)}(\mu\text{-Me})(\mu\text{-L}^*)\text{AlMe}_2]^+[\text{Me-MAO}]^-$ ($\text{L}^* = \text{Cl}$ or Me depending on the amount of MAO) via coordination of TMA to the cationic iron(II) center has been evidenced by paramagnetic ^1H NMR in toluene- d_8 after activation of 2,6-bis(imino)pyridine iron(II) chloride complexes with MAO.¹¹⁵⁻¹¹⁷ An equilibrium between active and inactive species identical to the one described above for Group 4 metallocenes was confirmed experimentally in the polymerization of ethylene.¹¹⁸

6.2 ESI-MS / UV-Vis investigations

6.2.1 Identification of $[\text{LFe-Me}]^+$ and $[\text{LFe-Cl}]^+$ as the activation products

The combination of electrospray ionization technique and tandem mass spectrometry (ESI-MS) is an attractive analytic method for the characterization of organometallic compounds thanks to its relatively soft ionization mode.¹¹⁹⁻¹²¹ ESI-MS was successfully applied to the study of metal complexes,¹²² metal catalyzed reaction mechanisms,^{123,124} polymerization catalysts,¹²⁵ and to high-throughput screening of homogeneous catalysis.^{126,127} The remarkable ability of electrospray to transfer ionic species from a sample solution to the gas phase was therefore found useful to investigate the composition of a sample solution of **1**/MAO by tandem mass spectrometry.

After a 63 $\mu\text{mol/L}$ sample of a **1**/MAO THF solution (MAO/Fe = 50) was infused in the ESI-MS, the obtained spectrum displayed a complicated and variable distribution of products (Figure 4), which could *a priori* be the consequence of the presence of air and moisture, as exemplified by the observation of the ligand peak at $m/z = 482$ (ligand + H^+). Nevertheless, a peak centered on $m/z = 552$ corresponding to the molar mass of the cationic 2,6-bis[1-(2,6-diisopropylphenylimino)ethyl]pyridine iron(II) methyl complex ($[\text{1-Me}]^+$) could be reproducibly observed. The fragmentation pattern of this ion was further studied by collision-induced dissociation (CID). A fragment at $m/z = 537$

correlates to the loss of a methyl group, followed by the loss of one isopropyl group from the ligand ($m/z = 494$).^{III} Analogously, the 572 ion corresponds to LFe^+-Cl ($[\mathbf{1}-\text{Cl}]^+$) (fragments obtained by CID at $m/z = 536$ ($[\mathbf{1}-\text{Cl}]^+-\text{Cl}$); 521 (-Me); 506 (-Me)).^{III,128,129}

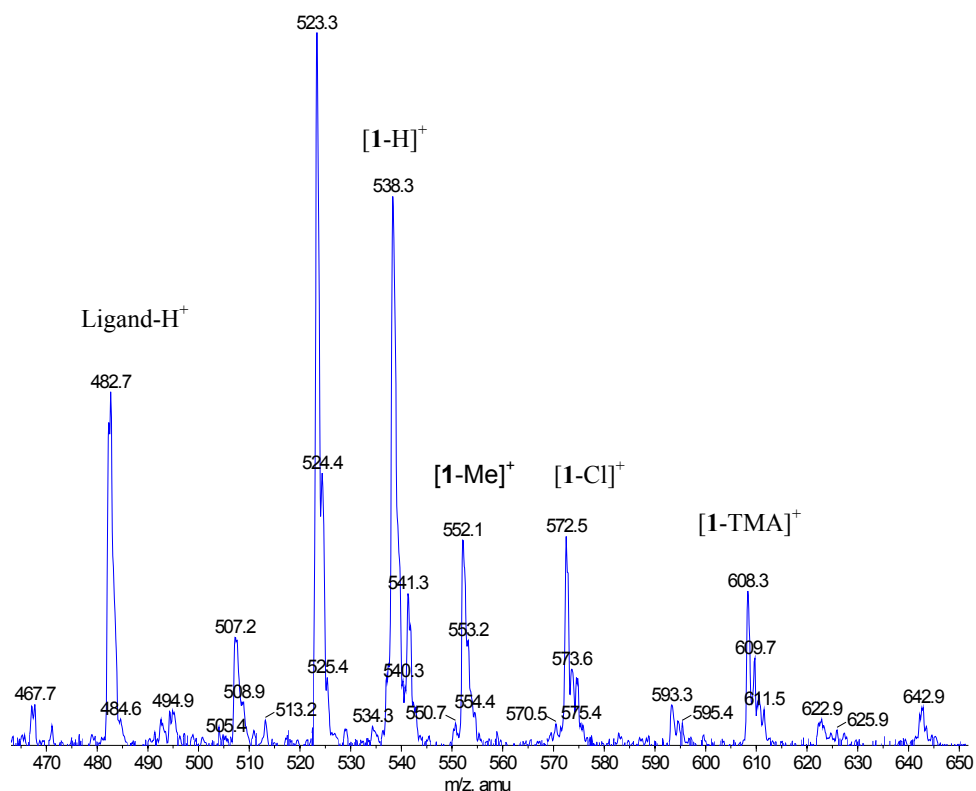


Figure 4. ESI-MS spectrum of **1**/MAO in THF.^{III}

The choice of THF as the solvent instead of the classical polymerization solvent toluene was not fortuitous. Indeed, as the polymerization of various (meth)acrylate monomers was performed in THF, it is conceivable that active species are also formed in this solvent.^{II} Furthermore, as a non-protic polar solvent, THF guarantees the total solubility of an ionic compound such as an iron(II) cationic complex bearing a weakly coordinating counter-anion. Finally and most importantly, donor molecules like THF are known to stabilize cationic metal alkyl¹³⁰⁻¹³² and hydride¹³² complexes by coordination. In the circumstances, the solid-state structure of $[\mathbf{1}-\text{Cl}]^+$ bearing the weakly coordinating anion SbF_6^- and of its cobalt analog could be determined by X-Ray diffraction as an

acetonitrile or THF adduct respectively.²⁴ Accordingly, after activation, $[\mathbf{1}\text{-Me}]^+$ and $[\mathbf{1}\text{-Cl}]^+$ are likely to be present in the solution as THF adducts, $[\mathbf{1}\text{-Me}]^+\cdot\text{THF}$ and $[\mathbf{1}\text{-Cl}]^+\cdot\text{THF}$, instead of the bimetallic Fe-Al complex observed in toluene.

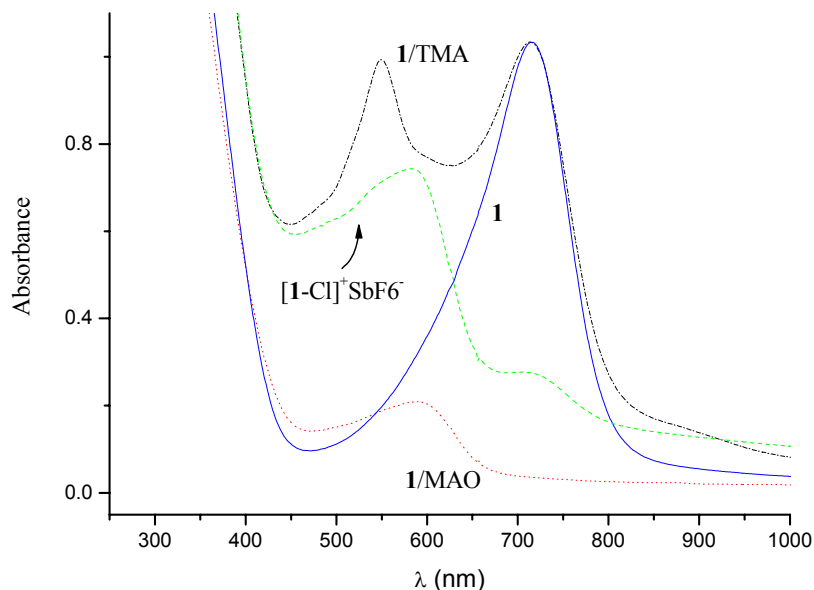
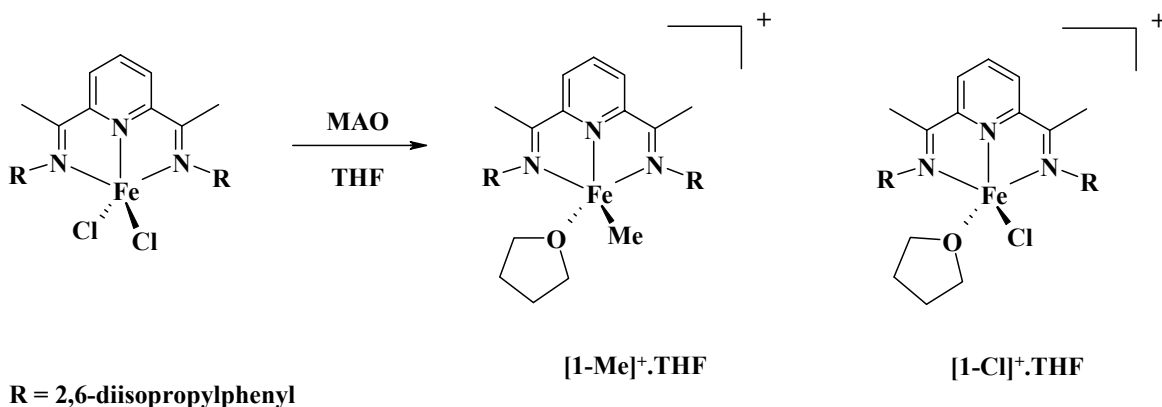


Figure 5. UV-Vis spectrum of **1**, **1/MAO**, **1/TMA** and $[\mathbf{1}\text{-Cl}]^+\text{SbF}_6^-$ in THF at room temperature. $[\text{Fe}] = 630 \mu\text{mol/L}$; $[\text{Al}]/[\text{Fe}] = 50$.

For this reason, the electronic spectrum of **1/MAO** in THF was investigated by UV-Vis spectroscopy (Figure 5). The position of absorption bands of transition metal complexes in the visible region being related to d-d transitions or to ligand to metal charge transfer band (LMCT),^{24,133,134} it is subject to variations depending on the electronic configuration at the metal center and therefore reflects the changes occurring in the coordination sphere of the metal.¹³⁴ In THF, **1** exhibits a deep royal blue color characterized by a broad absorption band in the visible region at 715 nm, which turns to light purple after the addition of 50 equivalents of MAO and steps aside to a unique less intense band at 588 nm, indicating that the entire catalyst precursor **1** was consumed during the reaction. In toluene, the faint broad absorption originating from **1/MAO** around 530 nm (in accordance with the value reported in the literature)²⁴ is red shifted to

a sharper band of a similar intensity at 599 nm after the addition of 10 equivalents of THF, indicating that two different species are present in toluene and in THF. In a control experiment, the UV-vis spectra of 2,6-bis[1-(2,6-diisopropylphenylimino)ethyl] pyridine iron(II) chloride hexafluoroantimonate acetonitrile adduct ($[\mathbf{1}\text{-Cl}]^+\cdot\text{CH}_3\text{CN}$, SbF_6^-) displayed a broad absorption at 584 nm in THF while it is reported to absorb at 540 nm in CH_2Cl_2 ,²⁴ evidencing that the signal arising from a five-coordinated 2,6-bis(imino)pyridine iron(II) cation is expected in the 580-590 nm area of the visible spectrum due to THF coordination.

It can then be concluded that the band at 588 nm from $\mathbf{1}/\text{MAO}$ illustrates the presence of the cationic species $[\mathbf{1}\text{-Me}]^+\cdot\text{THF}$ and $[\mathbf{1}\text{-Cl}]^+\cdot\text{THF}$ (Scheme 12). The application of a declustering potential in the ion source converts both adducts $[\mathbf{1}\text{-Me}]^+\cdot\text{THF}$ and $[\mathbf{1}\text{-Cl}]^+\cdot\text{THF}$ to free $[\mathbf{1}\text{-Me}]^+$ and $[\mathbf{1}\text{-Cl}]^+$.¹²⁵



Scheme 12. Activation products of $\mathbf{1}$ with MAO in THF: $[\mathbf{1}\text{-Me}]^+\cdot\text{THF}$ and $[\mathbf{1}\text{-Cl}]^+\cdot\text{THF}$.^{III}

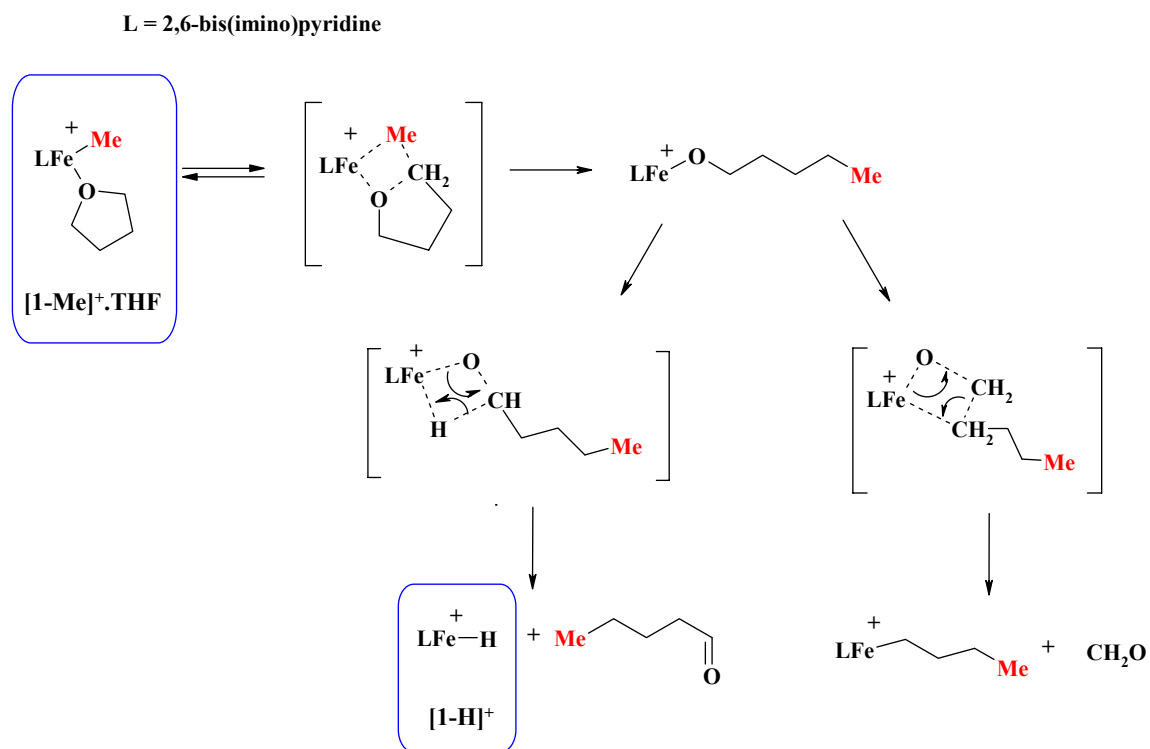
6.2.2 Other species detected with ESI-MS

Identification of iron hydride

The selection of the 538 ion, whose mass corresponds to $[\text{LFe-H}]^+$ ($[\mathbf{1}\text{-H}]^+$), in the first quadrupole and its fragmentation by CID gave signals at $m/z = 523$, and $m/z = 507$.^{III} It is then reasonable to deduce that the 523 (base peak) and 507 ions are formed by in-source CID of the 538 ion. When THF- d_8 was employed as the solvent instead of regular THF, a spectrum similar to Figure 4 was recovered, in particular the $[\mathbf{1}\text{-Me}]^+$ ion at $m/z =$

552, but a closer examination revealed some important differences. As a matter of fact, the peak corresponding to an isotopic ion of the 538 signal at $m/z = 539$ witnessed an intensity increase of about 10% compared to the normal run. Furthermore, signals at $m/z = 524$ and $m/z = 508$ were retrieved, matching a 1 amu increase of the 538, 523 and 507 masses. Accordingly, the origin of the 538 ion can, at least *to a certain extent*, be attributed to hydride transfer from THF, leading to the formation of $[1-H]^+$ ($[1-D]^+$ in THF- d_8).

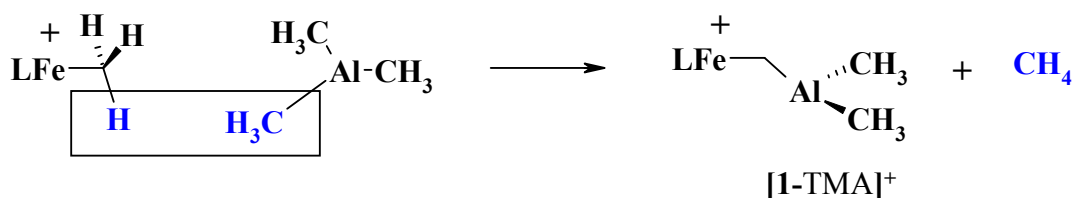
A rational explanation for the formation of $[1-H]^+$ involves the σ -bond metathesis of the THF C-O bond. Coordination of THF to the cationic metal center in $[1-Me]^+$ renders its α -carbon susceptible to nucleophilic attack from the methyl substituent, instigating the formation of a new cationic 2,6-bis(imino)pyridine iron(II) pentoxide *via* ring-opening of THF (Scheme 13). This iron alkoxide cation can subsequently undergo β -hydride and/or β -butyl transfer to the metal, at least in the gas phase, leading to the formation of iron hydride (major product) and iron butyl cations respectively.^{135,136}



Scheme 13. Proposed reaction mechanism of the ring opening of THF and subsequent β -hydride elimination leading to the formation of $[1-H]^+$.^{III}

Condensation with TMA

α -H transfer from a metallocenium-methyl bond to an Al-Me group is a well preceded side-reaction in MAO activated metallocene chemistry, resulting in the formation of a M-CH₂-Al bimetallic complex and the liberation of methane.^{37,137-139} The peak centered on $m/z = 608$ corresponds to the structure [LFe-CH₂-AlMe₂]⁺ ([1-TMA]⁺) and its CID gave two prominent fragments at $m/z = 593$ (loss of CH₃), and at $m/z = 578$ (loss of a second CH₃). Seemingly, [1-TMA]⁺ is produced by the reaction of [1-Me]⁺ with TMA, comparable to the α -H transfer reaction described above. It is however unclear whether the reaction occurs in solution or in the gas phase (Scheme 14).



L = 2,6-bis(imino)pyridine

Scheme 14. α -H transfer from [1-Me]⁺ to TMA leading to [1-TMA]⁺.^{III}

6.2.3 Summary

The detection of [1-Me]⁺ by ESI-MS is probably the first direct evidence of its existence as a “bare” coordinatively unsaturated cationic 2,6-bis(imino)pyridine iron(II) methyl complex. The detection of [1-Cl]⁺ also confirmed that at low MAO/Fe ratios, the activation reaction of **1** by MAO is not complete. Likewise, the presence in the ESI-MS spectrum of [1-H]⁺ constitutes a direct proof of the reality of this species, which is considered as a central reaction intermediate in the catalytic cycle of olefin polymerization. Its existence had previously only been deduced from the analysis of polymer end-groups,^{62,66} or indirectly verified from the addition of H₂ to a propylene polymerization reaction yielding to lowered molar mass and increased activity.¹⁴⁰ In any case, the presence of [1-H]⁺ is the consequence, at least partly, of THF coordination to [1-Me]⁺ in the catalyst solution. Based on the fact that the peaks at $m/z = 538$ and 523 corresponding to [1-H]⁺ are the most prominent peaks in the ESI-MS spectrum of

1/MAO, it can be assumed that in this particular case of low MAO/Fe ratio, polar donor solvent, and gas-phase mass spectrometry, $[\mathbf{1}\text{-Me}]^+\cdot\text{THF}$ is a major activation product of **1** in THF.

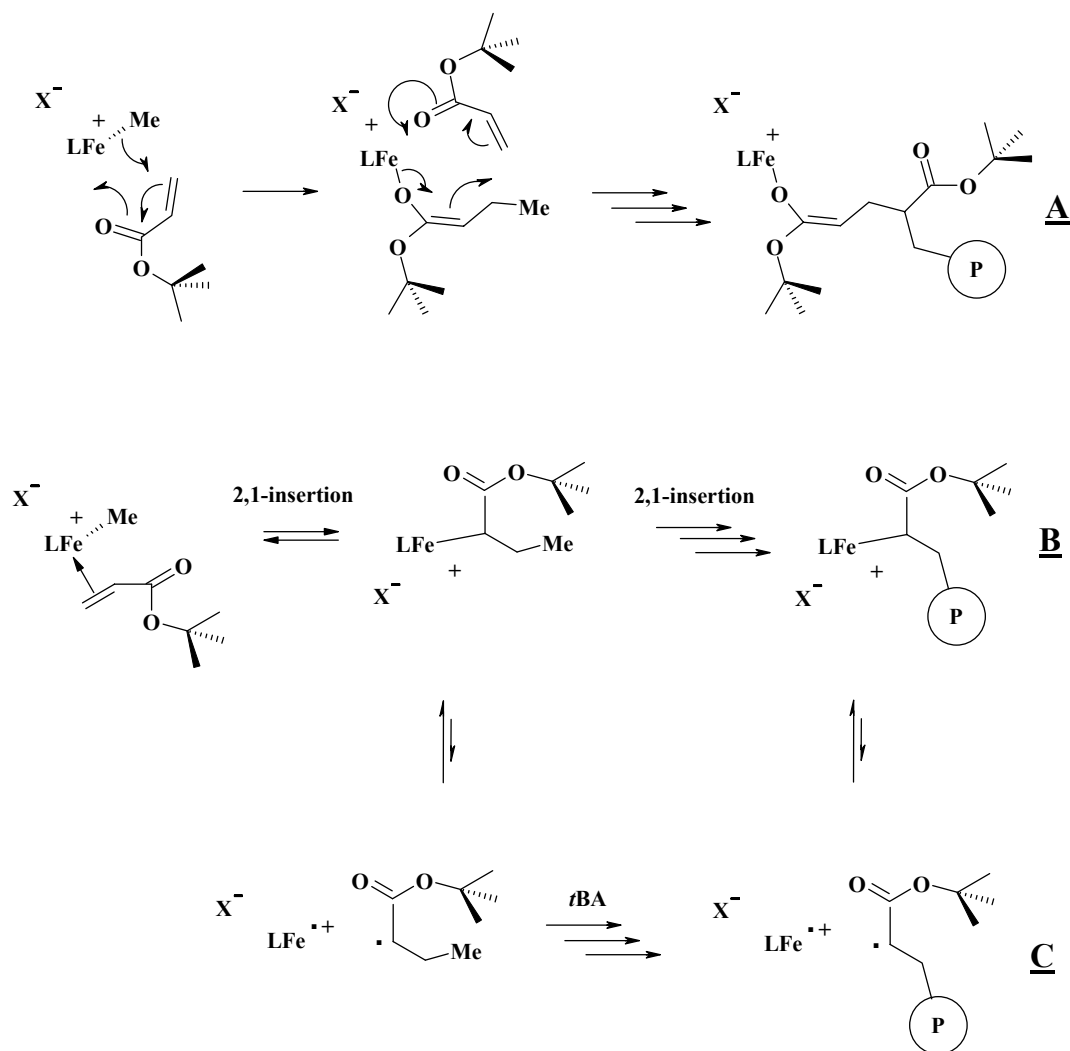
7 MAO Activated 2,6-Bis(imino)pyridine Iron Complexes for the Polymerization of Acrylates

7.1 Potential mechanisms

If structurally characterized stable paramagnetic iron(II) alkyl or halogeno alkyl complexes are known, though only recently reported,¹⁴¹⁻¹⁴³ they are generally prompt to decompose via reductive elimination,^{144,145} which significantly restricts the possibility to isolate and characterize catalytically active species. Moreover, in contrast to Group 4 metals⁷⁷ or palladium^{21,22} based acrylate polymerization systems, the paramagnetic nature of the 2,6-bis(imino)pyridine iron(II) catalyst thwarts any accurate NMR investigation of the events happening at the metal center when put in the presence of a monomer. Finally, the presence of MAO in the polymerization reaction prevents the utilization of radical scavengers such as galvinoxyl, classically used in disclosing radical mechanisms.^{146,147} Thus, distinguishing between radical, anionic-like and coordination/insertion polymerization mechanisms is rather challenging, and each propagating pathway has to be taken into consideration.

Accordingly, considering that the active form of the catalyst is $[\mathbf{1}\text{-Me}]^+$,^{III,24,65,110,118} and according to the different polymerization systems reviewed in paragraph 3.3, three different propagation pathway – anionic-like, coordination/insertion and metal-mediated radical – can be anticipated (Scheme 15). By analogy between single-component cationic monomethylated zirconocene catalysts⁷⁵⁻⁷⁷ and $[\mathbf{1}\text{-Me}]^+$, the possibility that the latter performs the polymerization of *t*BA through a similar pseudo-anionic type mechanism can be envisaged (Scheme 15/A). On the other hand, a vinylic monomer can π -coordinate to $[\mathbf{1}\text{-Me}]^+$ followed by insertion of the double-bond into the methyl-iron bond (Scheme 15/B);^{21,22,148} 2,1-insertion being favored to the detriment of 1,2-insertion according to

the charge distribution in the acrylate monomer. In a third alternative, similarly to what has been reported for iron,⁹² cobalt^{83,84} or palladium⁸⁵⁻⁸⁸ mediated radical polymerization, a propagating radical can be generated either from the original [1-Me]⁺ iron-methyl bond, or, more probably, after insertion of a first monomer for the simple reason that it provides a more stable radical (Scheme 15/C).



Scheme 15. Potential mechanisms for the polymerization of *t*BA with 1/MAO: GTP-like (A), coordination/insertion (B) and metal-mediated radical (C); X⁻ = [MAO-Me]⁻ or [MAO-X]⁻.^{IV}

7.2 Polymerization

7.2.1 Preliminary investigations

The original polymerization of *t*BA with a MAO activated 2,6-bis(imino)pyridine iron(II) chloride complex in our laboratory was undertaken with **1**/MAO in toluene. The successful polymerization encouraged us to investigate the influence of electronic and steric variations at the 2,6-bis(imino)pyridine ligand imine position towards the polymerization behavior: from constrained bulky phenyl (**1**, **2**) to “free rotating” aryl (**3**, **6**) and alkyl substituents (**4**, **5**). Preliminary polymerization results obtained with MAO activated **1-6** indicated that complexes **4** and **5** bearing alkyl substituents were more active than their aryl analogs, the less encumbered **4** being a better catalyst than **5**. Among the aryl substituted complexes, **2**, **3** and **6** exhibited a similar polymerization behavior, while **1** was the less active of the six catalysts. This lower activity has to be related to the steric protection provided around the iron center by the bulky isopropyl substituents (paragraph 3.2).

The catalytic activity and the molar mass of the polymers were found to increase with the monomer concentration.^I In contrast, raising the polymerization temperature provoked a drop of the molar mass with each catalyst **1-6**/MAO (Figure 6), without significant influence on the activity, indicating the occurrence of a chain-release process favored by higher temperatures.¹⁴⁹ On the other hand, even if syndiorich polymers were obtained in some cases, no significant influence of either the ligand structure, monomer concentration or polymerization temperature could be established. When THF was used as the solvent instead of toluene, higher conversions were obtained.^{II} This effect can be ascribed to a stabilizing effect of THF towards the propagating species (paragraphs 6.2.1 and 8.2). Due to its higher catalytic activity and to its simple ligand structure, the remainder of the polymerization studies was carried out with **4** as the catalyst precursor.

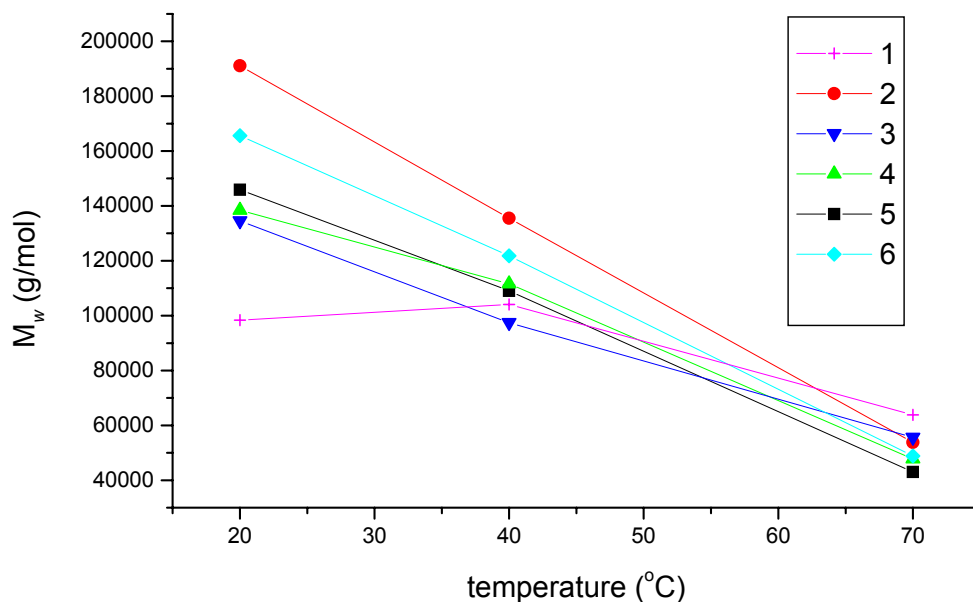


Figure 6. The effect of temperature on poly(*t*BA) M_n with **1-6**/MAO catalysts. Conditions: toluene; room temperature; [*t*BA] = 1.1 mol/L; MAO/Fe = 250; [Fe] = 0.33 mmol/L; reaction time = 24 hours.¹

7.2.2 Molar mass

The time dependence of both M_n and MWD was studied in toluene¹ (Figure 7/left) and THF¹¹ with **4**/MAO as the catalyst. The outcome indicates that M_n is independent of conversion, which confirms the existence of a chain release process (paragraph 7.2.1). According to the composition of the polymerization system, three transfer processes can be envisaged: β -hydride transfer to monomer, β -hydride transfer to metal and chain transfer to activator. As the molecular weight increases proportionally to the monomer concentration (paragraph 7.2.1), β -hydride transfer to monomer can be excluded. The influence of the MAO concentration on the polymer chain length was then examined by varying the MAO/Fe ratio. In toluene, M_n is independent from the MAO concentration as it stays nearly constant and centered around 100 kg/mol (Figure 7/right). Transfer to aluminum is not the main chain-transfer process in this solvent. On the contrary, the same

experiment done in THF showed that transfer to aluminum is effective as M_n diminished with increasing MAO/Fe values.^{II}

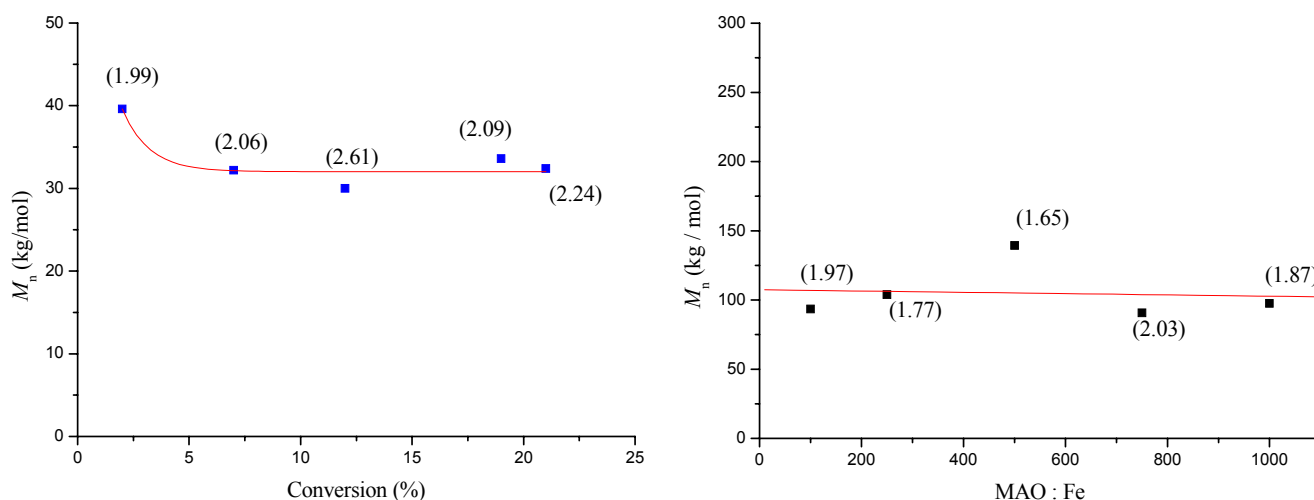


Figure 7. M_n dependence on conversion (left) and on MAO/Fe ratio (right). MWD is indicated between brackets. Conditions: toluene; room temperature; $[tBA] = 1.1$ mol/L; MAO/Fe = 250; $[Fe] = 63 \mu\text{mol/L}$; reaction time = 2 hours.^{IV}

7.2.3 Polymer end-groups

Identification of the polymer chain-ends was achieved by means of ^{13}C (Figure 8) and ^{13}C DEPT 135 from a low molar mass *t*BA polymer ($M_n = 4000$ g/mol, MWD = 1.63) synthesized by using a low concentration of monomer ($[tBA] = 0.2$ mol/L, $[Fe] = 63 \mu\text{mol/L}$ and MAO/Fe = 250). The signals arising from the main polymer chain are indicated with capital letters **A-E** in Figure 8.¹⁵⁰ The minor signals labeled **a-h** are tokens of end-groups and/or structural defects. The saturated region of the ^{13}C NMR spectrum clearly shows two peaks, **a** and **b**, at 12 ppm and 26 ppm respectively. A third peak **c** is found at 46 ppm. The ^{13}C DEPT 135 spectrum indicates that **a** and **c** correspond to a primary or tertiary carbon, while **b** corresponds to a secondary carbon. According to the ^{13}C NMR data found in the literature, an ethyl substituent at the α -carbon of a methyl ester is characterized by signals at 13.85 ppm ($\text{CH}_3\text{CH}_2\text{CHCO}_2\text{Me}$), 20.36 ppm ($\text{CH}_3\text{CH}_2\text{CHCO}_2\text{Me}$) and 43.38 ppm ($\text{CH}_3\text{CH}_2\text{CHCO}_2\text{Me}$), while a methyl substituent

gives signals at 18.02 ppm ($\text{CH}_3\text{CHCO}_2\text{Me}$) and 37.77 ppm ($\text{CH}_2\text{CHCO}_2\text{Me}$).¹⁵¹ It therefore seems likely that the saturated chain ends are mainly composed of ethyl groups ($\text{CH}_3\text{CH}_2\text{CH}(\text{CO}_2\text{tBu})$ -polymer), indicating a favored 2,1-insertion of the monomer (paragraph 7.1).

As for the signal **d** at 128 ppm, it denotes the presence of insaturations in the polymer chain. Unsaturated chain-ends have been observed with CCT^{82,93-95} and in metal-mediated radical polymerization of polar monomers.^{83,84,87,88,92} Unsaturated chain-ends are usually considered as evidence for a β -hydride transfer process, in the circumstances β -hydride transfer to the metal.

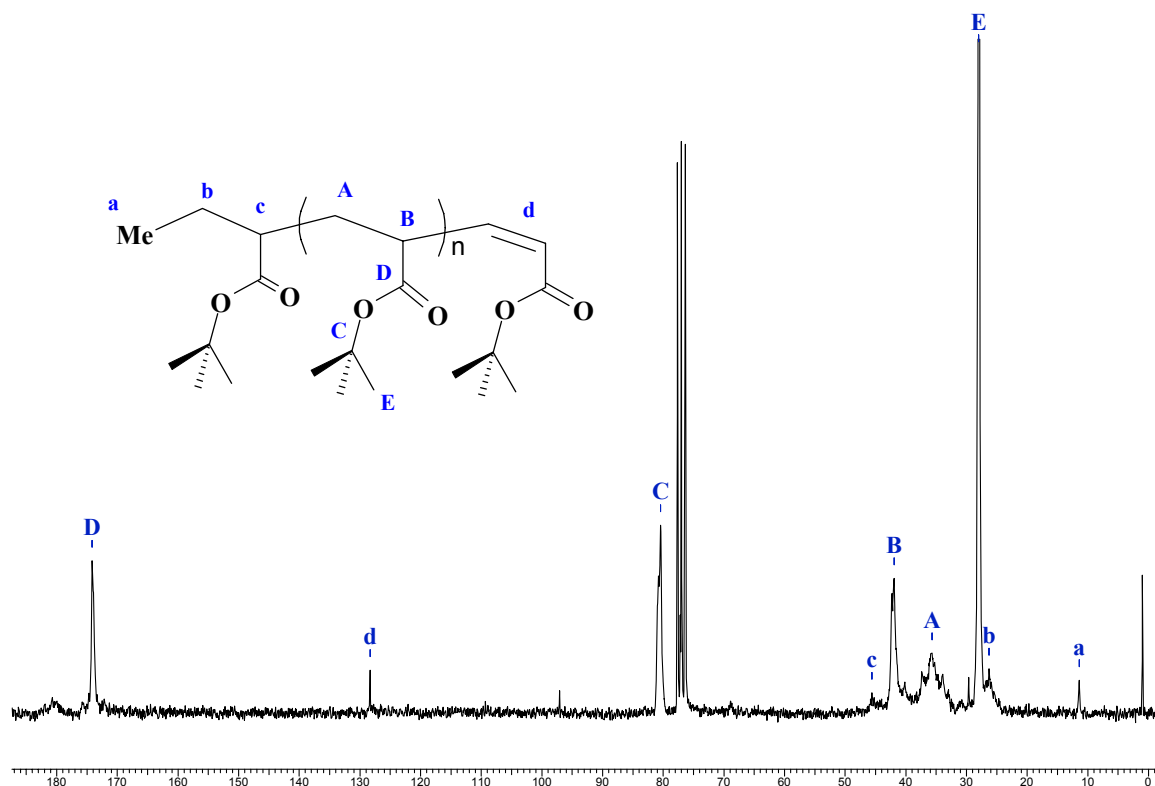


Figure 8. 50MHz ^{13}C NMR spectrum of poly(*t*BA) in CDCl_3 at 25°C. $M_n = 4000$ g/mol; MWD = 1.63. Conditions: [tBA] = 0.2 mol/L; MAO/Fe = 250; [Fe] = 63 $\mu\text{mol/L}$; reaction time = 2 hours.^{IV}

7.2.4 Polymerization kinetics

Kinetic analysis is a powerful tool for the comprehension of reaction mechanisms, particularly in the case of catalytic processes. The rate law of *t*BA polymerization

catalyzed by 4/MAO in toluene was thus established by monitoring the monomer consumption with GC. The resulting logarithmic curves corresponding to the iron precatalyst, MAO and *t*BA are displayed in Figure 9 (paragraph 4.3).

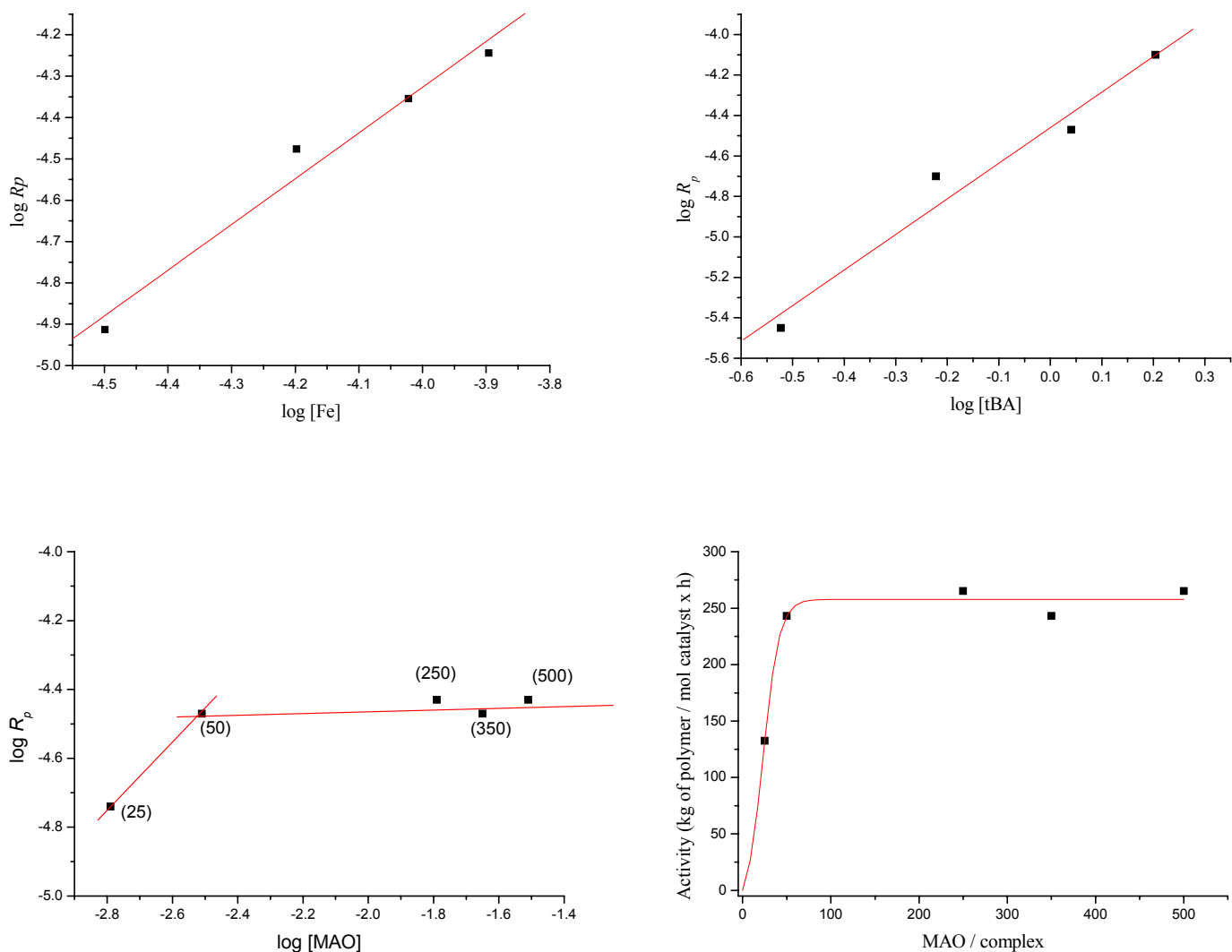


Figure 9. Logarithmic variations of the *t*BA polymerization rate vs. complex (up left), monomer (up right) and co-catalyst (down left) concentration (toluene, room temperature, 1 hour reaction time); and influence of the MAO/Fe ratio on the *t*BA polymerization activity (toluene, room temperature, $[t\text{BA}] = 1.1 \text{ mol/L}$; $[\text{Fe}] = 63 \mu\text{mol/L}$, 1 hour reaction time).^{IV}

The rate order corresponding to the concentration of **4** was found to be of 1.1 ± 0.1 , thus close to 1, indicating that a single active species is involved in the polymerization process (Figure 9, up left). This excludes the participation of a second metal center acting as a monomer activator, as it has been described for the bimetallic GTP-like mechanism.^{68,69} In the case of MAO, two different trends were retrieved (Figure 9, down left): below a MAO to Fe ratio of 50, the rate order with respect to MAO is sensibly equal to one, while at higher ratios, it is close to zero. Plotting the polymerization activity vs. MAO/Fe ratio shows a sharp increase until a plateau of maximal activity is reached for MAO/Fe values above 50 (Figure 9, down right). This indicates that the proportion of active species increases proportionally to the concentration of MAO until an optimum MAO/Fe ratio of 50, corresponding to a steady-state concentration in active species.^{149,152} Furthermore, this zero-order dependence on aluminum species indicates that at higher concentrations, aluminum does not act as a monomer activating agent.^{8,153}

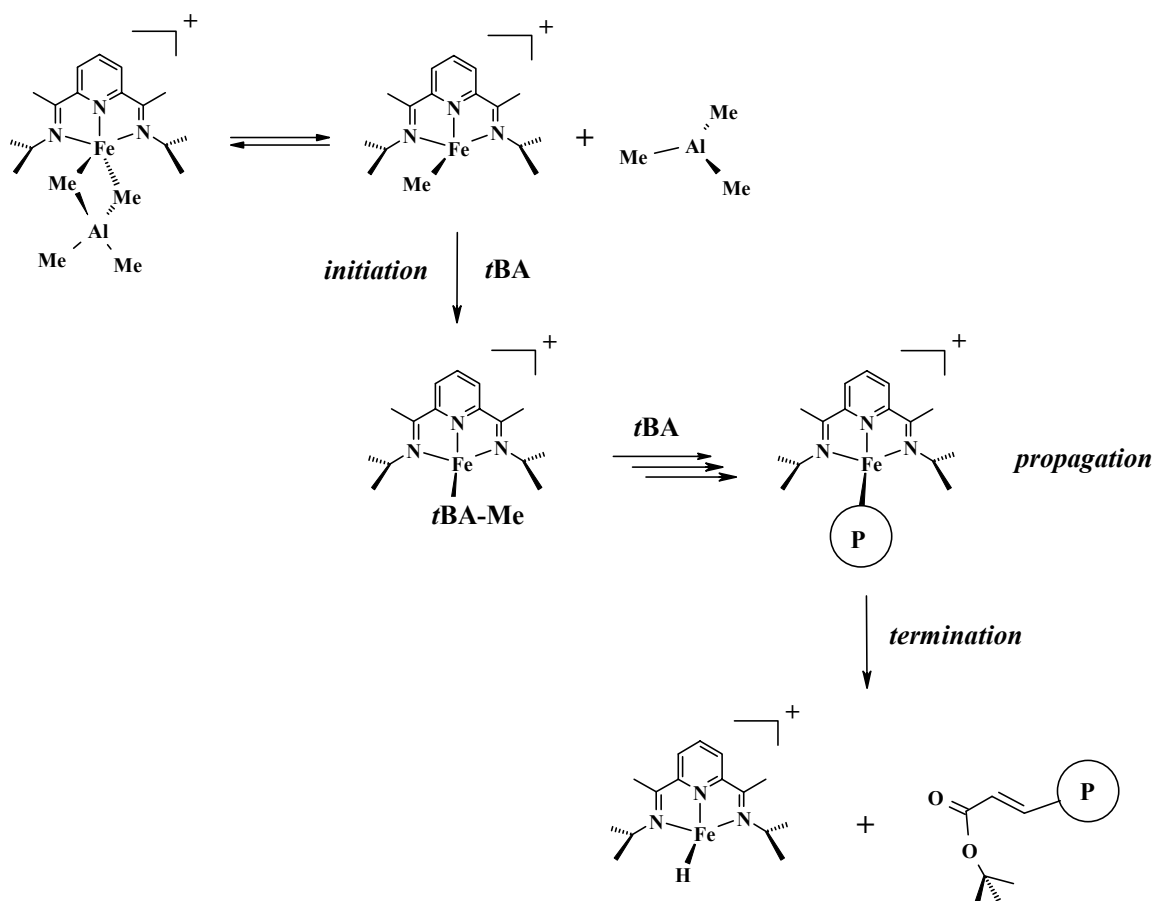
The kinetic order on *t*BA is an unexpected value of 1.7 ± 0.2 , *i.e.* 1.5 to 1.9 monomer units are involved in the rate determining step of the propagation (Figure 9, up right). The observation of a higher reaction order on monomer concentration is known for transition metal catalyzed propylene polymerization^{149,154-156} – though the exact cause is not well understood and still subject to debate. A common feature between most of the different models established to rationalize this observation is that a dormant/less active state of the catalyst is transformed into a highly active one by interaction with a monomer. Likewise, the observation of higher reaction orders with respect to monomer have been reported in free radical polymerization and attributed to the participation of the monomer in the initiation stage.¹⁵⁷

The overall rate law for the polymerization is given by equation (1) for MAO/Fe < 50 and by equation (2) for MAO/Fe > 50:

$$R_p = [\text{Fe}]^{1.1 \pm 0.1} [\text{Al}]^{1 \pm 0.1} [\text{tBA}]^{1.7 \pm 0.2} \quad (1)$$

$$R_p = [\text{Fe}]^{1.1 \pm 0.1} [\text{Al}]^0 [\text{tBA}]^{1.7 \pm 0.2} \quad (2)$$

The equilibrium between active and inactive forms of the catalyst described in paragraph 6.1 for the 1/MAO catalyzed polymerization of ethylene can be extrapolated here: as kinetic investigations endorse the participation of an additional *t*BA monomer in the propagation process, it is conceivable that initiation occurs when the iron catalyst is trapped in its highly reactive monometallic form ($[LFe-Me]^+$) by a first *t*BA, followed by propagation with further incoming monomers. Deactivation can occur by TMA coordination, and propagation is terminated by chain release, for instance via a β -hydride transfer elimination (7.2.3). Independently from the propagation mechanism, the higher reaction order with respect to monomer concentration can be explained by the dependence of the initiation rate on the monomer concentration (Scheme 16).



Scheme 16. Schematic representation of the polymerization catalyzed by 1/MAO.

7.2.5 UV-Visible Spectroscopy.

The modifications occurring at the iron center after activation with MAO in toluene and subsequent monomer addition were examined by UV-Vis spectroscopy (Figure 10). The addition of 100 molar equivalents of MAO to a toluene solution of **4** induced a color change from blue to light orange, which was expressed by a shift of the LMCT band from 730 nm to 490 nm. This new broad LMCT absorption is attributable to the bimetallic Fe-Al cation similar to what is observed with **1**/MAO.^{117,III} When a large excess of *t*BA was added, the **4**/MAO 490 nm absorption disappeared and new absorption maxima in the 470 nm region vaguely distinguishable due to the overlap of the strong UV peak, and around 550 nm were observed.

With the purpose of clarifying the propagating species structure, a model reaction was carried out by adding 2 equivalents of lithium *tert*-butyl α -lithiopropenolate to a toluene solution of **4** under the same experimental conditions that prevails during the polymerization,^{158,159} followed after 4 hours by 1 equivalent of N,N-dimethylanilinium tetrakis(perfluorophenyl)borate.^{IV} The resulting deep orange solution displayed a UV-Vis spectrum alike the *t*BA polymerization solution, with a broad absorption at 470-490 nm and a shoulder around 550 nm (Figure 10), which were assigned to the presence of a new product (**7**, Scheme 17).¹⁶⁰ The close resemblance of both the polymerization and **7** spectra suggests that the propagating species in the polymerization reaction is structurally related to **7**, and that the counter-anion, MAO-X⁻ (X = Me or Cl) or B(C₆F₅)₄⁻, has no significant influence on the electronic properties of the iron cation. Unfortunately, due to its high instability, **7** could not be isolated.

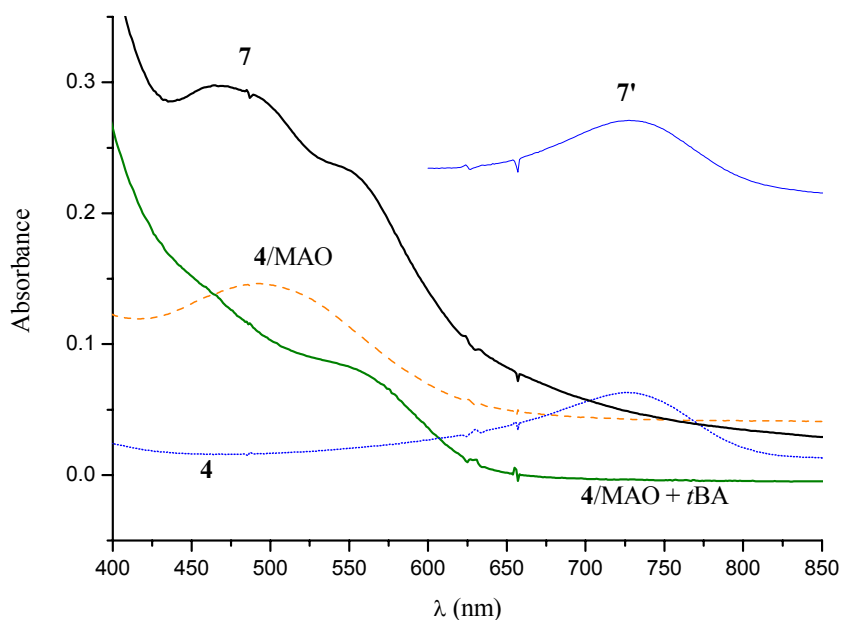
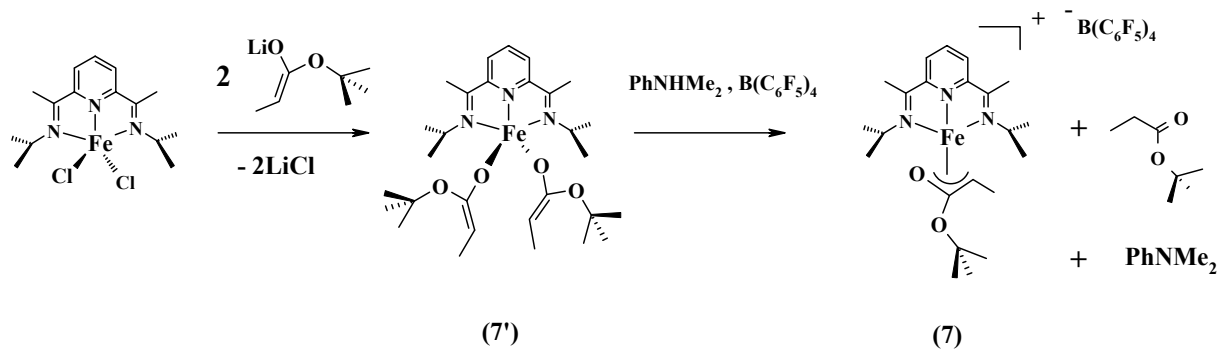


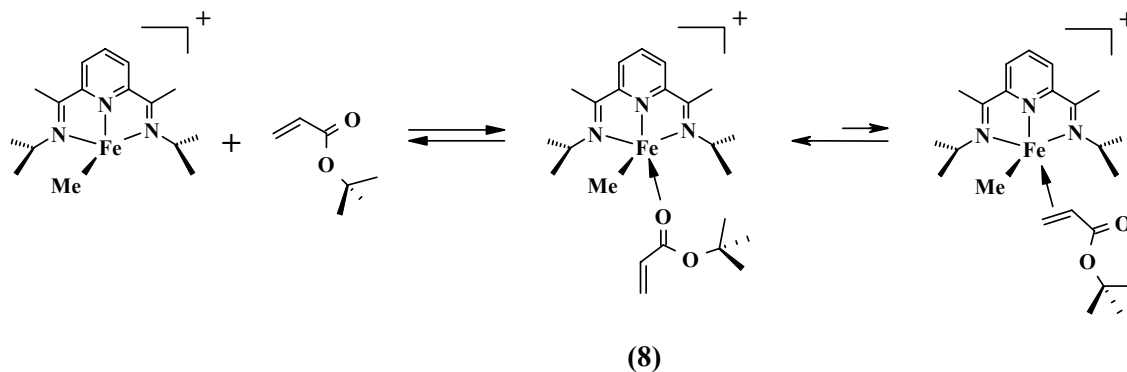
Figure 10. UV-vis absorption spectra of **4**, **4/MAO**, of the polymerization solution (**4/MAO** + *t*BA) and of the model compounds **7'** and **7** in toluene, at room temperature. Conditions: [Fe] = 630 μ mol/L; MAO/Fe = 100; [tBA] = 1.1 mol/L.^{IV}



Scheme 17. Formation of **7**.^{IV}

When *tert*-butyl propionate was added to a toluene solution of **4/MAO**, a similar spectrum was retrieved, with absorption maxima at 470 and 550 nm. Thanks to its similarity to the experiments conducted with **1/MAO** (paragraph 6.2.1), this spectrum can be related to TMA displacement from the iron center by O-coordination of the ester

function. Therefore, the appearance of a shoulder at higher wavelength in the absorption spectrum of the polymerization solution is attributable to a five-coordinated iron cationic complex bearing an O-bonded *t*BA (**8**, Scheme 18).^{161,162}



Scheme 18. Bonding of *t*BA to $[1\text{-Me}]^+$ leading to **8**.

7.2.6 Copolymerization with 1-hexene

Copolymerization was performed in toluene with *t*BA and 1-hexene as the comonomers. After a two-hour reaction, a small amount of an amorphous transparent material was recovered, and the conversion of *t*BA was lower than in homopolymerization reactions.^{IV} When *t*BA was used in excess, the polymer glass transition temperature (T_g) was significantly lowered compared to homopoly(*t*BA) (14°C instead of 50°C), while no T_g could be detected when excess of 1-hexene was employed. The ¹³C NMR spectrum depicted in Figure 11 displays characteristic peaks from both poly(*t*BA)¹⁵⁰ and poly(1-hexene).¹⁶³ The enlargement of the carbonyl carbon area around 174 ppm displays a shoulder at 174.8 ppm which is absent in the homopoly(*t*BA) spectrum (Figure 8). This shoulder has previously been attributed to the feature of acrylate-hexene enchainment, verifying that the copolymerization reaction provides a copolymer instead of a blend of homopolymers.^{59,85,87} Considering the relative size of both signals at 174 and 174.8 ppm, **1**/MAO produces a random copolymer. Indeed, the 174.8 ppm signal would hardly be detected from a block copolymer or an acrylate chain-terminated poly(1-hexene) as described by Brookhart.^{21,22} Consequently, according to

paragraph 3.4, the production of a random copolymer rules against a GTP-like mechanism.

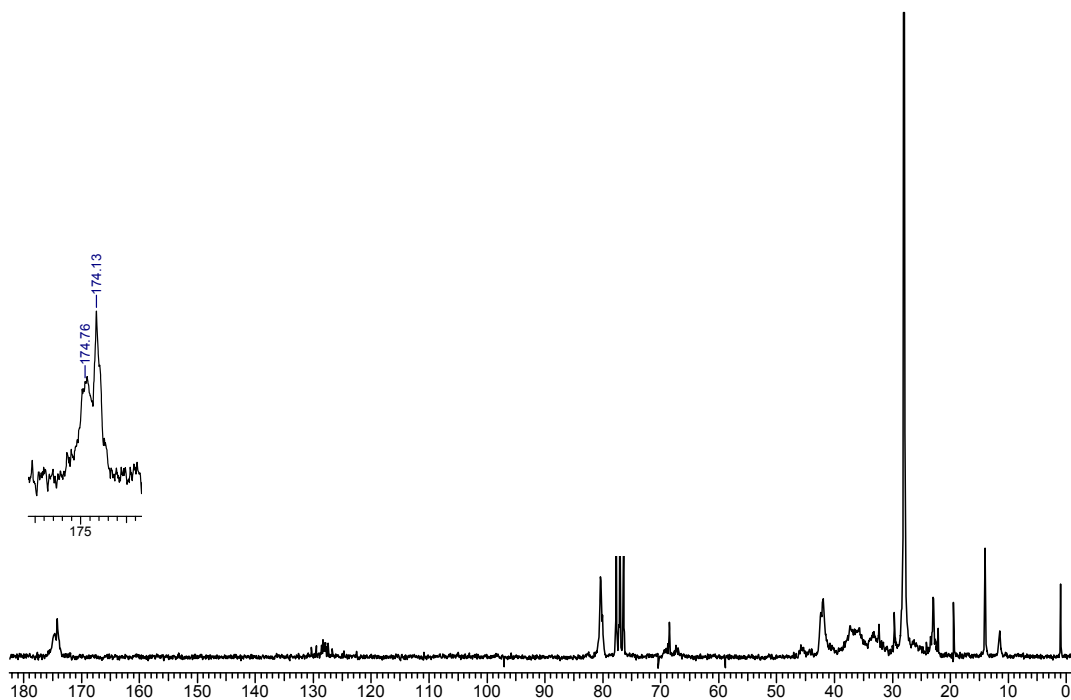


Figure 11. 50MHz ¹³C NMR spectrum of poly(*t*BA-co-1-hexene) in CDCl₃ at 25°C. $M_n = 1300$ g/mol; PDI = 3.5. Conditions: MAO/Fe = 250; [Fe] = 63 μmol/L; reaction time = 2 hours. The area corresponding to the carbonyl carbon is enlarged.^{IV}

7.3 Concluding remarks about the polymerization mechanism

7.3.1 Initiation

After the active form of 4/MAO – [LFe-Me]⁺ – has been trapped by a monomer, two potential initiation modes have to be taken into account: iron-methyl bond homolysis leading to a radical propagation, or insertion of a coordinated *t*BA into the iron-methyl bond resulting in either radical or coordination/insertion mechanism. In the latter case, initiation takes place if the *t*BA inserts into the metal-carbon bond, which necessitates the formation of a π bound Fe-*t*BA complex. Given that the cationic iron has an intrinsic

electrophilic nature, it is likely that an acrylate monomer bearing two oxygen donor atoms will σ -coordinate to the metal via its polar functionalities at the expense of a π -bonding mode from which insertion can occur, as confirmed by UV-Vis. π -Bonding is thus expected to be attained through the establishment of an O/ π isomerization equilibrium (Scheme 18). The regio-chemistry of the subsequent insertion is confirmed to occur in a 2,1 mode on account of the polymer ethyl end-group evidenced by ^{13}C and DEPT 135 NMR (paragraph 7.2.3).

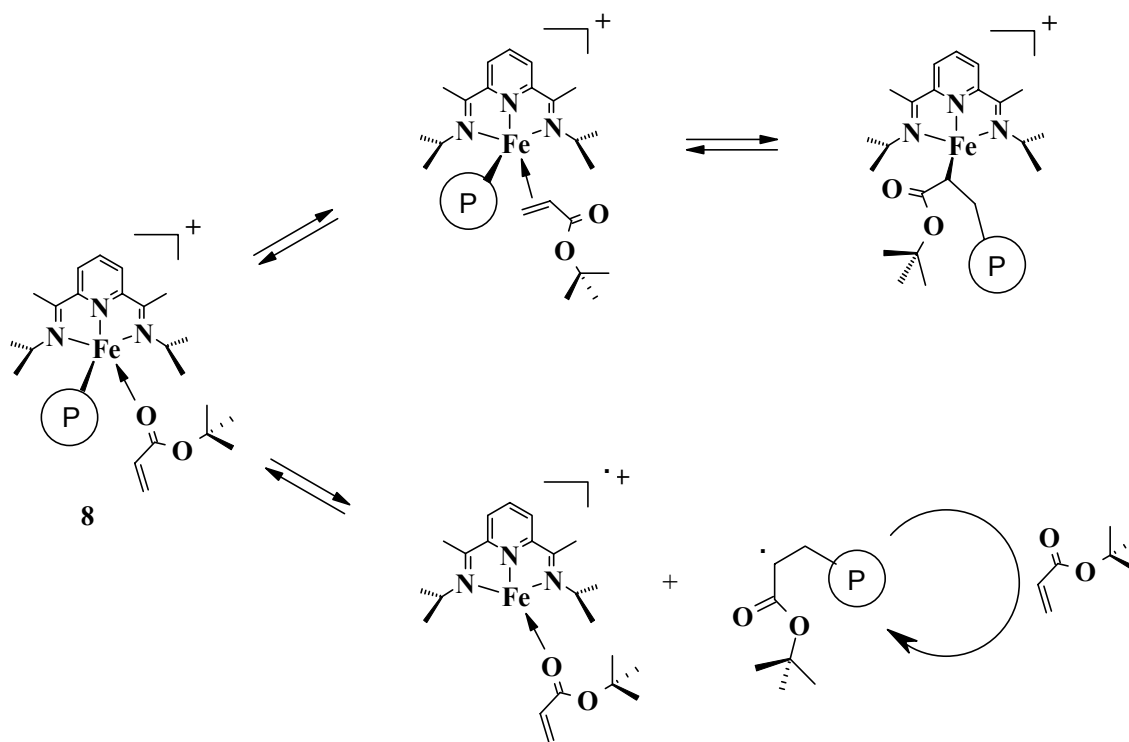
7.3.2 Propagation

The difficulty of assigning a propagation pathway for late transition metal catalyzed polymerization of polar monomers is well exemplified by the polymerization of acrylonitrile (AN) with the neutral coordinatively saturated low-spin bis-(2,2'-dipyridine)iron diethyl ((biPy) $_2$ (Et) $_2$ Fe) catalyst, which was originally reported to occur via a “coordinated anionic polymerization” in the mid 1970s^{49,164}. Almost thirty years later, a radical¹⁶⁵ and an anionic¹⁶⁶ polymerization were claimed almost simultaneously by two different groups for the same system.

Considering a metal-mediated radical pathway, iron-carbon bond homolysis is known in the organometallic chemistry of iron, but it mainly concerns the redox couple Fe(III)/Fe(II), particularly in iron porphyrin complexes¹⁶⁷⁻¹⁶⁹ and CCT polymerization of (meth)acrylates or styrene.^{82,93-95} Spontaneous reduction of iron(II) bearing a covalently bonded carbon substituent was reported for the reaction of phenyl tris(3-*tert*-butylpyrazolyl)borato iron(II) methyl with carbon monoxide (CO), yielding an unexpected 15-electron iron(I) complex bearing a CO ligand.¹⁷⁰ The isolation of this iron(I) species points out the possibility for a cationic iron(II) complex bearing a tridentate nitrogen ligand to undertake metal-carbon bond homolysis in the presence of a stabilizing donor ligand.

In view of this, two different events can occur after O-coordination of a monomer to the active form of the catalyst (**8**, Scheme 19): rearrangement from O- to π -bonding and subsequent insertion of the *t*BA into the iron-carbon bond (coordination/insertion pathway), or iron-carbon bond homolysis engendering a metal-centered iron(I) radical stabilized by coordination with *t*BA and a transient propagating radical which can

reversibly combine back to **8** (metal-mediated radical polymerization). As both the observation of a higher reaction order relative to monomer and the existence of an unsaturated chain-end can take place in coordination/insertion and radical polymerizations, differentiating between the two propagation modes is at present hardly achievable. Random copolymerization with α -olefins can as well be achieved by either of the two mechanisms.

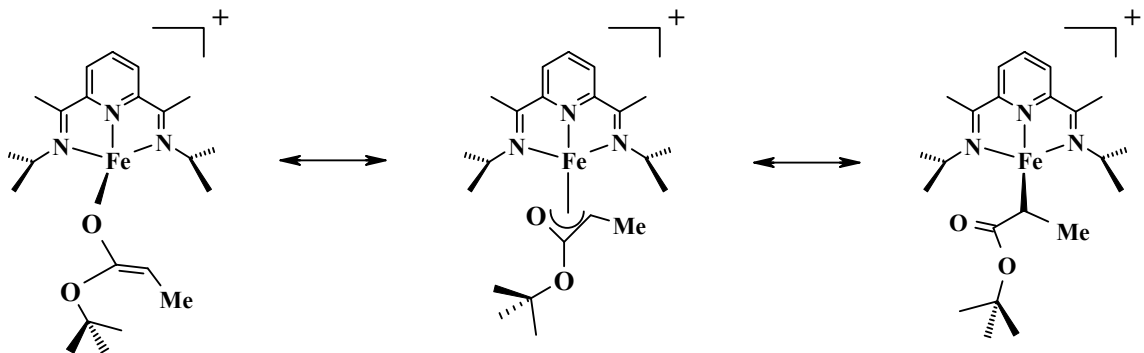


Scheme 19. Proposed propagation pathways from **8**.^{IV}

7.3.3 Nature of the propagating species

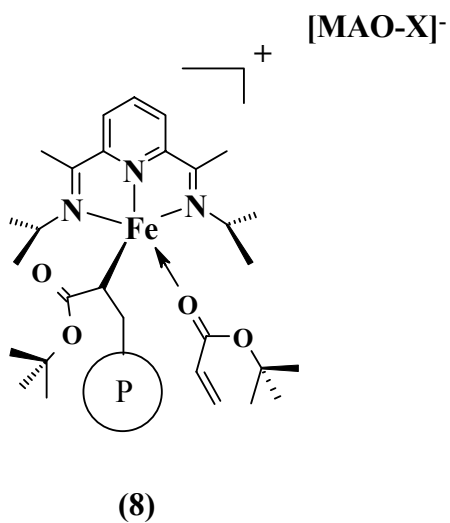
Metal ester enolates can display three different bonding modes: C-bonding, O-bonding or η^3 -oxoallyl bonding (Scheme 20). Comparison of electropositive early transition metal enolates with less electron deficient palladium ester enolates emphasizes the fact that the former prefer metal-oxygen bonds,^{76,171,172} whereas the latter compounds preferably exhibit metal-carbon bonds.^{173,174} A glance at Pauling's electronegativity values shows that iron (1.8) is situated in between group 4 metals (1.3-1.5) and palladium

(2.2). In this sense, either bonding mode depicted in Scheme 20 can be expected for a cationic iron complex.



Scheme 20. Bonding modes in an ester enolate of **4**.^{IV}

Nevertheless, in the present case, the occurrence of β -hydride transfer to the metal corroborates a C-bound polymer. The propagation mechanism also privileges a C-bonding mode as the intermediacy of a C-bond complex is required in both metal-mediated radical and coordination/insertion pathways. It can then be proposed that the propagating species is a five-coordinated cationic 2,6-bis(imino)pyridine iron(II) complex bearing a C-bond polymer chain and an O-coordinated *t*BA (**8**, Scheme 21).



Scheme 21. Proposed structure for the propagating species **8**.

8 Diphosphine Iron(II) Chloride Complexes

In spite of the fact that the ability of diphosphine complexes of iron(II) halogenide to catalyze carbon-carbon bond formation when combined with an alkyl aluminum co-catalyst was demonstrated via the co-dimerization of 1,3-butadiene and ethylene into 1,4-hexadiene in the mid-1960s,¹⁷⁵ the use of phosphine based transition metal complexes as polymerization (*i.e.* multiple subsequent carbon-carbon bond formation) catalyst precursors is scarcely described in the literature. Few examples of alkylaluminum or alkyl aluminum activated phosphine complexes of nickel, iron or cobalt have been reported to provide the polymerization of styrene,¹⁷⁶ norbornene¹⁷⁷ and 1,3-butadiene.¹⁷⁸

The straightforward synthesis,^V relative robustness and commercial availability of the ligands encouraged us to investigate diphosphine complexes of iron(II) as alternatives to 2,6-bis(imido)pyridine iron(II) complexes in the polymerisation of acrylate monomers (Chart 2.).

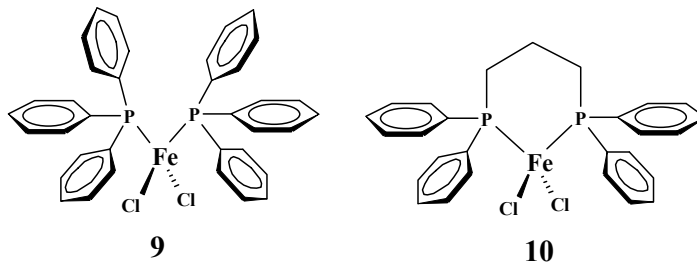


Chart 2.^V

8.1 Polymerization of MA with iron(II) catalysts

Originally, we employed an iron(II) chloride complex bearing two triphenylphosphine (PPh_3) ligands ($(\text{PPh}_3)_2\text{FeCl}_2$, **9**) to examine the capacity of phosphine based late metal complexes in polymerizing acrylate monomers when combined with MAO. In preliminary experiments in THF, **9**/MAO revealed a higher polymerization activity than **4**/MAO.^{II} This prompted us to investigate the behavior of a bridged diphosphine ligand, 1,3-bis(diphenylphosphino)propane (DPP), complex of

iron(II) chloride (DPPFeCl₂, **10**) in acrylate polymerization, as multidentate phosphine ligands are known to provide alternative activities and selectivities compared to monodentate ligands.

8.1.1 Ligand effect

The polymerization of MA in toluene at different temperatures permitted the observation of a ligand effect on both the polymerization activity and the obtained molar masses (Figure 12). Indeed, while the activity increases with the temperature, the values displayed by **9**/MAO and **10**/MAO at room temperature and at 70°C suggest that higher activities are reached with PPh₃ as the ligand than with (DPPP). The difference is more pronounced when the molar mass is considered as the M_n vs. T curve displays two different trends according to the ligand (Figure 12/right). However, in each case the obtained polymers are fully atactic.

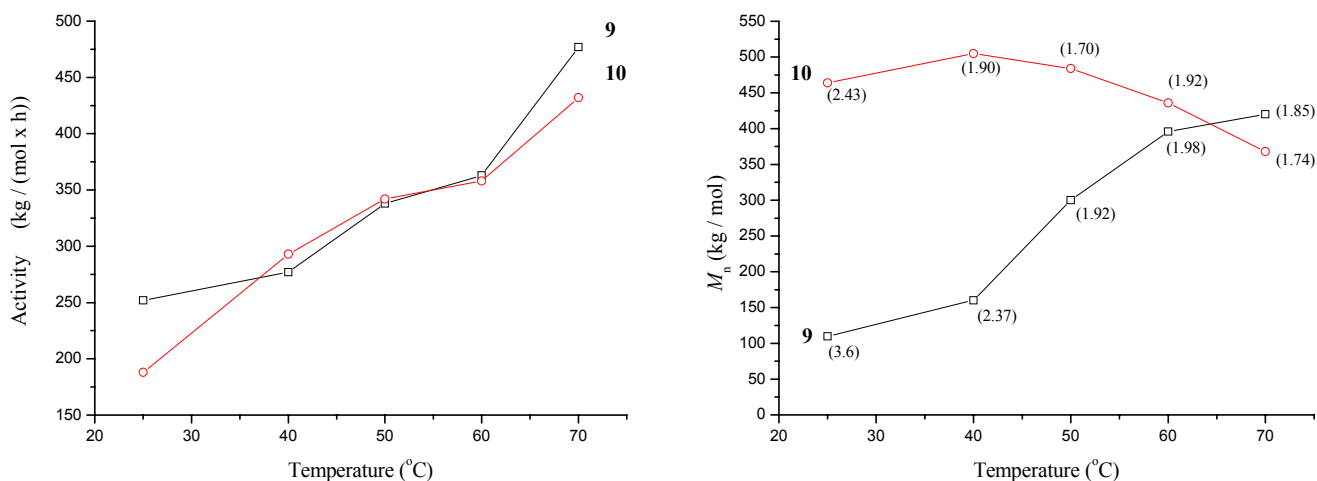


Figure 12. Polymerization activity (left) and molar mass (right) variations with temperatures for **9**/MAO and **10**/MAO. Conditions: [MMA] = 7.4 mol/L; MAO/Fe = 250; [Fe] = 0.27 mmol/L; reaction time = 3 hours.^V

8.1.2 Chain transfer

The influence of the cocatalyst concentration on the molar mass of the obtained polymers was investigated at room temperature with **9**/MAO and **10**/MAO by varying the

MAO/Fe ratio from 50 to 1000 (Figure 13). It was seen that M_n is directly affected by the MAO/Fe ratio as it drops with increasing concentration of aluminium in a similar manner for both catalysts. Therefore, differing from **4**/MAO (7.2.1), polymerization of MA catalyzed by **9-10**/MAO processes with chain-transfer to aluminum at room temperature. The increase of M_n observed at higher temperatures (Figure 12/right) signifies that as the temperature increases, propagation is favored to the detriment of termination. In the case of **10**/MAO, M_n starts to decrease above 50°C. At this limit temperature it is reasonable to think that another chain release phenomenon becomes prevalent, resulting in a lessening of the molar mass, but a further increase of the activity. Unfortunately, the high molar mass of the obtained polymers prevents any unambiguous end-group analysis by infrared or NMR spectroscopy, and the nature of this second chain release process remains unclear.

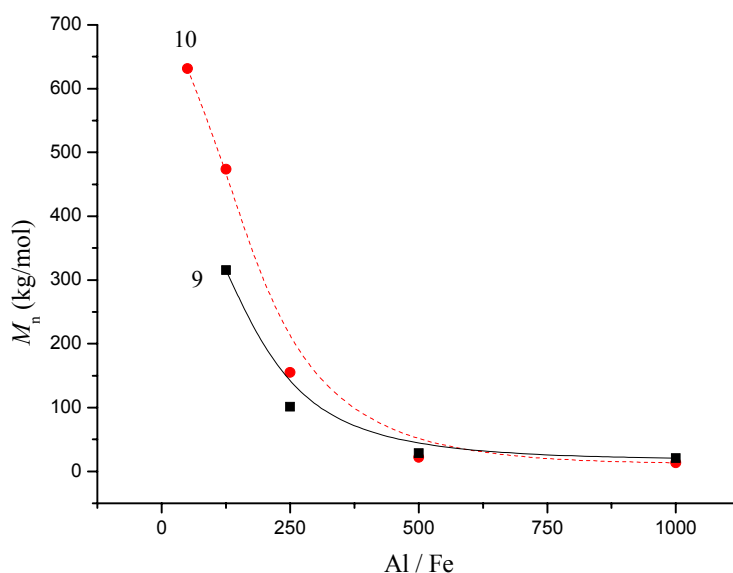


Figure 13. Influence of MAO/Fe ration on M_n for **9**/MAO and **10**/MAO.^V

8.2 Nature of the active species

Iron(II) complexes of dihalogeno(diphosphine) have been reported to undergo alkylation when reacted with alkyl aluminum compounds.¹⁷⁹ It is then reasonable to

assume that when a toluene solution of complexes **9** or **10** is treated with an excess of MAO, a cationic monomethylated iron complex LFe^+-Me ($L = (PPh_3)_2$ or DPPP) is formed.^{III}

In fact, the activity vs. MAO/Fe curve parallels the observations reported for MAO activated metallocene catalyzed α -olefin polymerization (Figure 14/left).¹⁴⁹ At a lower MAO/Fe ratio, a low activity is obtained, due to the insufficient amount of activator leading to incomplete activation of the iron precursor. Then, similar to what was observed with **4**/MAO (7.2.4), a maximum concentration of active species corresponding to an optimum MAO/Fe ratio is reached. A marked difference with **4**/MAO is that the activity drops at higher MAO/Fe values, seemingly due to an excess of aluminum species acting as deactivating agents through MAO coordination to the vacant coordination site, or by formation of a bimetallic Fe-Al complex with TMA. Furthermore, when free PPh_3 was added to a **9**/MAO polymerization solution, a decay of the catalytic activity was observed (Figure 14/right). Considering the intrinsic Lewis base nature of phosphine ligands, an acid-base interaction between the Lewis base PPh_3 and a Lewis acidic LFe^+-Me active species blocking the access to a vacant coordination site can be credited for this decay.

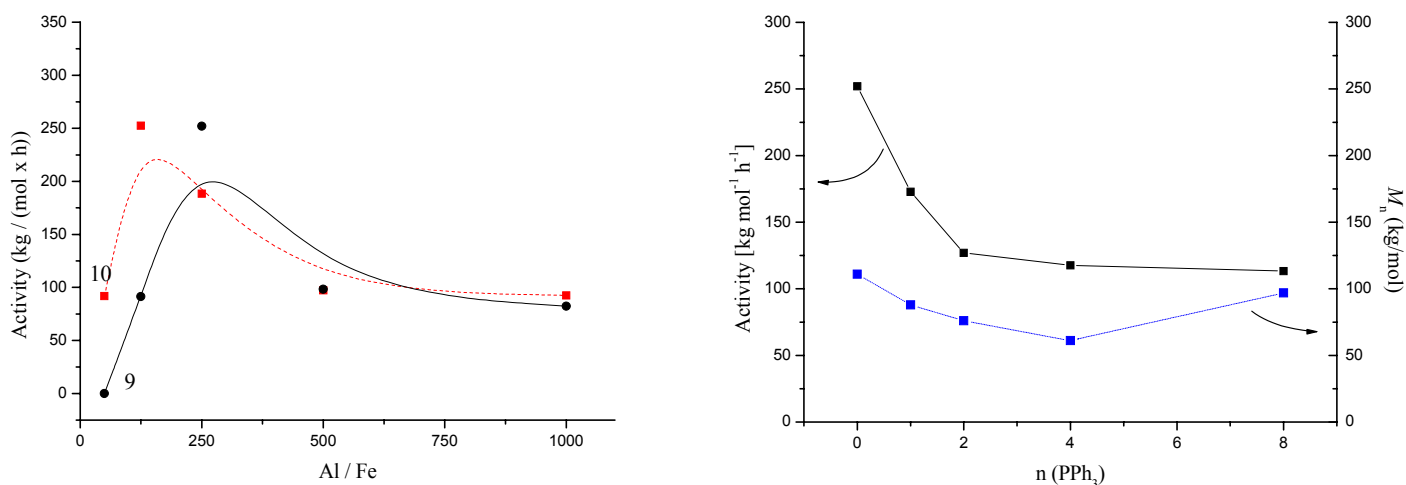


Figure 14. Activity vs. MAO/Fe ratio for **9**/MAO and **10**/MAO (left) and influence of an added PPh_3 on activity and molar mass for **9**/MAO (right).

These results agree with the findings made for 2,6-bis(imino)pyridine based iron complexes that when MAO is added to a toluene solution of the iron complex, a vacant coordination site is created at the iron center where monomers coordinate. The availability of this site controls the polymerization activity.

9 Conclusion

The work presented in this thesis started with the observation that MAO activated iron(II) complexes bearing either tridentate 2,6-Bis(imino)pyridine or bidentate diphosphine ligands could efficiently promote the homopolymerization of acrylate monomers.

A consistent part of this study was devoted to the understanding of the catalyst activation process and the interactions between its active form and donor species. The coordinatively unsaturated cationic iron(II) methyl $[1\text{-Me}]^+$ was identified as one of the products resulting from the MAO activation of 2,6-bis[1-(2,6-diisopropylphenylimino)ethyl]pyridine iron(II) chloride (**1**) in solution. This cationic complex is claimed to be the catalytically active species in olefin polymerization and despite the fact that its existence had been postulated, it had never been observed spectroscopically before. Complementary UV-Visible spectroscopy studies showed that four-coordinated cationic 2,6-bis(imino)pyridine iron(II) methyl species are inclined to form a five-coordinated adduct in the presence of a donor ligands like THF or tert-butyl esters.

Detailed homopolymerization studies were undertaken in order to get a better insight into the polymerization mechanism, and the random copolymerization of tert-butyl acrylate with 1-hexene was achieved with the MAO activated 2,6-bis[(1-isopropylimido)ethyl]pyridine iron dichloride catalyst (**4**/MAO). Despite the fact that the necessity for monomer coordination to the metal centre was demonstrated with both nitrogen and phosphorous based catalysts, a definitive statement about the intrinsic polymerisation mechanism must be restrained as discriminating between radical, anionic-like or coordination/insertion is far from being straightforward at the present stage. The

identification of the intimate mechanism would need an accurate determination of the relative monomer incorporation in (*t*BA-co-1-hexene) copolymers,^{146,147} or a precise determination of the iron-carbon bond energy in species like **9** in order to establish the feasibility of a bond homolysis. Three situations can then be considered. At higher values, homolytic cleavage of the iron-carbon bond is an improbable event and insertion of the monomer into the iron-carbon bond via a classical concerted migratory insertion should be favored. At low energy values, iron-carbon bond homolysis should prevail to the detriment of recombination, leading to a free radical polymerization, entailing chain transfer reactions as well as rapid termination of the chain growth via recombination and/or disproportionation. Between these two extreme cases, at an optimum bond energy, homolysis competes with fast reversible recombination of the polymer radical with the Fe(I) metal-centered radical, ensuring a low concentration of propagating radicals and providing a transition metal-mediated controlled radical polymerization process.

References.

- (1) About chain termination and chain transfer in free-radical polymerization, see Odian, G. *Principles of Polymerization*, 3rd ed.; Wiley: New York **1991**; p 241-259.
- (2) About chain termination and chain transfer in anionic polymerization, see Odian, G. *Principles of Polymerization*, 3rd ed.; Wiley: New York **1991**; p 403-407.
- (3) Szwarc, M. *Nature* **1956**, *178*, 1168-1169.
- (4) Szwarc, M.; Levy, M.; Milkovich, R. *J. Am. Chem. Soc.* **1956**, *78*, 2656-2657.
- (5) Colombani, D. *Prog. Polym. Sci.* **1997**, *22*, 1649-1720.
- (6) Goto, A.; Fukuda, T. *Prog. Polym. Sci.* **2004**, *29*, 329-385.
- (7) Vlček, P.; Lochmann, L. *Prog. Polym. Sci.* **1999**, *24*, 793-873.
- (8) Baskaran, D. *Prog. Polym. Sci.* **2003**, *28*, 521-581.
- (9) Collins, S.; Ward, D. W. *J. Am. Chem. Soc.* **1992**, *114*, 5460-5462.
- (10) Soga, K.; Deng, H.; Yano, T.; Shiono, T. *Macromolecules* **1994**, *27*, 7938-7940.
- (11) Deng, H.; Shiono, T.; Soga, K. *Macromolecules* **1995**, *28*, 3067-3073.
- (12) Yasuda, H.; Yamamoto, H.; Yokota, K.; Miyake, S.; Nakamura, A. *J. Am. Chem. Soc.* **1992**, *114*, 4908-4910.
- (13) Yasuda, H.; Yamamoto, H.; Yamashita, M.; Yokota, K.; Nakamura, A.; Miyake, S.; Kai, Y.; Kanehisa, N. *Macromolecules* **1993**, *26*, 7134-7143.
- (14) Boffa, L. S.; Novak, B. M. *Macromolecules* **1994**, *27*, 6993-6995.
- (15) Giardello, M. A.; Yamamoto, Y.; Brard, L.; Marks, T. J. *J. Am. Chem. Soc.* **1995**, *117*, 3276-3277.
- (16) Boffa, L. S.; Novak, B. M.; *Chem. Rev.* **2000**, *100*, 1479-1493.
- (17) Britovsek, G. J. P.; Gibson, V. C.; Wass, D. F. *Angew. Chem. Int. Ed.* **1999**, *38*, 428-447.
- (18) Ittel, S. D.; Johnson, L. K.; Brookhart, M. *Chem. Rev.* **2000**, *100*, 1169-1203.
- (19) Gibson, V. C.; Spitzmesser, S. K. *Chem. Rev.* **2003**, *103*, 283-315.
- (20) Younkin, T. R.; Connor, E. F.; Henderson, J. I.; Friedrich S. K.; Grubbs, R. H.; Bansleben, D. A. *Science* **2000**, *287*, 460-462.
- (21) Johnson, L. K.; Mecking, S.; Brookhart, M. *J. Am. Chem. Soc.* **1996**, *118*, 267-268.
- (22) Mecking, S.; Johnson, L. K.; Wang, L.; Brookhart, M. *J. Am. Chem. Soc.* **1998**, *120*, 888-899.
- (23) DiRenzo G. M.; White, P. S.; Brookhart M. *J. Am. Chem. Soc.* **1996**, *118*, 6225-6234.
- (24) Britovsek, G. J. P.; Gibson, V. C.; Spitzmesser, S. K.; Tellmann, K. P.; White, A. J. P.; Williams, D. J. *J. Chem. Soc., Dalton Trans.* **2002**, *6*, 1159-1171.

-
- (25) Endo, K.; Inukai, A.; Otsu, T. *Macromol. Rapid Commun.* **1994**, *15*, 893-896.
- (26) Coutinho, F. M. B.; Costa, M. A. S.; Monteiro, L. F.; de Santa Maria, L. C. *Polym. Bull.* **1997**, *38*, 303-309.
- (27) Ihara, E.; Fujimura, T.; Yasuda, H.; Maruo, T.; Kanehisa, N.; Yasushi, K. *J. Polym. Sci. Part A: Polym. Chem.* **2000**, *38*, 4764-4775.
- (28) Endo, K.; Yamanaka, Y. *Macromol. Rapid Commun.* **2000**, *21*, 785-787.
- (29) Endo, K.; Inukai, A. *Polym. Int.* **2000**, *49*, 110-114.
- (30) Carlini, C.; Martinelli, M.; Galletti, A. M.; Sbrana, G. *J. Polym. Sci., Part A: Polym. Chem.* **2003**, *41*, 1716-1724.
- (31) Carlini, C.; Martinelli, M.; Raspolli Galletti, A. M.; Sbrana, G. *J. Polym. Sci. Part A: Polym. Chem.* **2003**, *41*, 2117-2124.
- (32) He, X.; Yao, Y.; Luo, X.; Zhang, J.; Liu, Y.; Zhang, L.; Wu, Q. *Organometallics* **2003**, *22*, 4952-4957.
- (33) Ihara, E.; Maeno, Y.; Yasuda, H. *Macromol. Chem. Phys.* **2001**, *202*, 1518-1523.
- (34) Nata, G.; Pino, P.; Mazzanti, G.; Giannini, U. *J. Am. Chem. Soc.* **1957**, *79*, 2975-2976.
- (35) Breslow, D. S.; Newburg, N. R. *J. Am. Chem. Soc.* **1957**, *79*, 5072-5073.
- (36) Sinn, H.; Kaminsky, W.; Vollmer, H. J.; Woldt, R. *Angew. Chem., Int. Ed. Engl.* **1980**, *19*, 390-392.
- (37) Kaminsky, W. *J. Polym. Sci. Part A: Polym. Chem.* **2004**, *42*, 3911-3921.
- (38) Chen, E. Y. X.; Marks, T. J. *Chem. Rev.* **2000**, *100*, 1391-1434.
- (39) Jüngling, S.; Mülhaupt, R. *J. Organomet. Chem.* **1995**, *497*, 27-32.
- (40) Ziegler, K. GB Patent Application 713081, 1954; *Chem. Abstr. Numb.* 49:18368.
- (41) Wilke, G. In *Ziegler Catalysts, Recent Scientific Innovations and Technological Improvements*; Fink, G., Mülhaupt, R., Brintzinger, H. H., Eds.; Springer-Verlag: Berlin Heidelberg 1995; p 1-14.
- (42) Cotton, F. A. *Chem. Rev.* **1955**, *55*, 551-594.
- (43) Cossee, P. *J. Catal.* **1964**, *3*, 80-88.
- (44) Arlman, E. J.; Cossee, P. *J. Catal.* **1964**, *3*, 99-104.
- (45) Yamamoto, A.; Morifuji, K.; Ikeda, S.; Saito, T.; Uchida, Y.; Misono, A. *J. Am. Chem. Soc.* **1965**, *87*, 4652-4653.
- (46) Saito, T.; Uchida, Y.; Misono, A.; Yamamoto, A.; Morifuji, K.; Ikeda, S. *J. Am. Chem. Soc.* **1966**, *88*, 5198-5201.
- (47) Yamamoto, A.; Ikeda, S. *J. Am. Chem. Soc.* **1967**, *89*, 5989-5990.

-
- (48) Yamamoto, A.; Morifuji, K.; Ikeda, S.; Saito, T.; Uchida, Y.; Misono, A. *J. Am. Chem. Soc.* **1968**, *90*, 1878-1883.
- (49) Yamamoto, A.; Shimizu, T.; Ikeda, S. *Makromol. Chem.* **1970**, *136*, 297-302.
- (50) Yamamoto, A.; Shimizu, T.; Ikeda, S. *Polym. J.* **1970**, *1*, 171-180.
- (51) Yamamoto, T.; Yamamoto, A.; Ikeda, S. *Bull. Chem. Soc. Jpn.* **1972**, *45*, 1104-1110.
- (52) Yamamoto, T.; Yamamoto, A.; Ikeda, S. *Bull. Chem. Soc. Jpn.* **1972**, *45*, 1111-1117.
- (53) Yamamoto, A. *J. Chem. Soc., Dalton Trans.* **1999**, 1027-1037.
- (54) Yamamoto, A. *J. Organomet. Chem.* **2004**, *689*, 4499-4510.
- (55) Kukral, J.; Abele, A.; Müller, G.; Rieger, B. In *Late Transition Metal Polymerization Catalysis*; Rieger, B., Baugh, L. S., Kacker, S., Striegler, S. Eds.; Wiley-VCH: Weinheim 2003; p 27-28.
- (56) Johnson, L. K.; Killian, C. M.; Brookhart, M. *J. Am. Chem. Soc.* **1995**, *117*, 6414-6415.
- (57) Killian, C. M.; Tempel, D. J.; Johnson, L. K.; Brookhart, M. *J. Am. Chem. Soc.* **1996**, *118*, 11664-11665.
- (58) Gottfried, A. C.; Brookhart, M. *Macromolecules* **2003**, *36*, 3085-3100.
- (59) Drent, E.; van Dijk, R.; van Ginkel, R.; van Oort, B.; Pugh, R. I. *Chem. Commun.* **2002**, 744-745.
- (60) Small, B. M.; Brookhart, M.; Bennett, A. M. A. *J. Am. Chem. Soc.* **1998**, *120*, 4049-4050.
- (61) Britovsek, G. J. P.; Gibson, V. C.; Kimberley, B. S.; Maddox, P. J.; McTavish, S. J.; Solan, G. A.; White, A. J. P.; Williams, D. J. *Chem. Commun.* **1998**, 849-850.
- (62) Britovsek, G. J. P.; Bruce, M.; Gibson, V. C.; Kimberley, B. S.; Maddox, P. J.; Mastroianni, S.; McTavish, S. J.; Redshaw, C.; Solan, G. A.; Strömberg, S.; White, A. J. P.; Williams, D. J. *J. Am. Chem. Soc.* **1999**, *121*, 8728-8740.
- (63) Small, B. L.; Brookhart, M. *J. Am. Chem. Soc.* **1998**, *120*, 7143-7144.
- (64) Deng, L.; Margl, P.; Ziegler, T. *J. Am. Chem. Soc.* **1999**, *121*, 6479-6487.
- (65) Khoroshun, D.; Musaev, D. G.; Vreven, T.; Morokuma, K. *Organometallics* **2001**, *20*, 2007-2026.
- (66) Small, B. L.; Brookhart, M. *Macromolecules* **1999**, *32*, 2120-2130.
- (67) Webster, O. W.; Hertler, W. R.; Sogah, D. Y.; Farnham, W. B.; RajanBabu, T. V. *J. Am. Chem. Soc.* **1983**, *105*, 5706-5708.
- (68) Collins, S.; Ward, D. G.; Suddaby, K. H. *Macromolecules* **1994**, *27*, 7222-7224.
- (69) Li, Y.; Ward, D. G.; Reddy, S. S.; Collins, S. *Macromolecules* **1997**, *30*, 1875-1883.

-
- (70) Giardello, M. A.; Yamamoto, Y.; Brard, L.; Marks, T. J. *J. Am. Chem. Soc.* **1995**, *117*, 3276-3277.
- (71) Cui, Chunming, Shafir, A.; Reeder, C. L.; Arnold, J. *Organometallics* **2003**, *22*, 3357-3359.
- (72) Nodono, M.; Tokimitsu, T.; Makino, T. *Macromol. Chem. Phys.* **2003**, *204*, 877-884.
- (73) Cameron, P. A.; Gibson, V. C.; Graham, A. J. *Macromolecules* **2000**, *33*, 4329-4335.
- (74) Chen, Y. X. E.; Metz, M. V.; Li, L.; Stern, C. L.; Marks, T. J. *J. Am. Chem. Soc.* **1998**, *120*, 6287-6305.
- (75) Frauenrath, H.; Keul, H.; Höcker, H. *Macromolecules* **2001**, *34*, 14-19.
- (76) Bolig, A. D.; Chen, E. Y. X. *J. Am. Chem. Soc.* **2004**, *126*, 4897-4906.
- (77) Rodriguez-Delgado, A.; Chen, E. Y. X. *Macromolecules* **2005**, *38*, 2587-2594.
- (78) Colombani, D. *Prog. Polym. Sci.* **1997**, *22*, 1649-1720.
- (79) Kamigaito, M.; Ando, T.; Sawamoto, M. *Chem. Rev.* **2001**, *101*, 3689-3745.
- (80) Matyjaszewski, K.; Xia, J. *Chem. Rev.* **2001**, *101*, 2921-2990.
- (81) Gridnev, A. *J. Polym. Sci. Part A: Polym. Chem.* **2000**, *38*, 1753-1766.
- (82) Gridnev, A. A.; Ittel, S. D. *Chem. Rev.* **2001**, *101*, 3611-3659.
- (83) Wayland, B. B.; Poszmik, G.; Mukerjee, S. L. *J. Am. Chem. Soc.* **1994**, *116*, 7943-7944.
- (84) Wayland, B. B.; Basickes, L.; Mukerjee, S.; Wei, M.; Fryd, M. *Macromolecules* **1997**, *30*, 8109-8112.
- (85) Tian, G.; Boone, H. W.; Novak, B. M. *Macromolecules* **2001**, *34*, 7656-7663.
- (86) Sun, H.; Shen, Q.; Peng, X.; Yang, M. *Catal. Lett.* **2002**, *80*, 11-18.
- (87) Elia, C.; Elyashiv-Barad, S.; Sen, A.; López-Fernández, R.; Albéniz, A. C.; Espinet, P. *Organometallics* **2002**, *21*, 4249-4256.
- (88) Albéniz, A. C.; Espinet, P.; López-Fernández, R. *Organometallics* **2003**, *22*, 4206-4212.
- (89) Arafa, I. M.; Shin, K.; Goff, H. M. *J. Am. Chem. Soc.* **1988**, *110*, 5228.
- (90) Guillard, R.; Kadish, K. M. *Chem. Rev.* **1988**, *88*, 1121-1146.
- (91) Riordan, C. G.; Halpern, J. *Inorg. Chim. Acta* **1996**, *243*, 19-24.
- (92) Oh, Y.; Swenson, D.; Goff, H. M. *Bull. Korean Chem. Soc.* **2003**, *24*, 167-172.
- (93) Gibson, V. C.; O'Reilly, R. K. O.; Reed, W.; Wass, D. F.; White, A. J. P.; Williams, D. J. *Chem. Commun.* **2002**, 1850-1851.
- (94) Gibson, V. C.; O'Reilly, R. K.; Wass, D. F.; White, A. J. P.; Williams, D. J. *Macromolecules* **2003**, *36*, 2591-2593.
- (95) O'Reilly, R. K.; Gibson, V. C.; White, A. J. P.; Williams, D. J. *Polyhedron* **2004**, *23*, 2921-2928.

-
- (96) Endo, K. *Macromol. Chem. Phys.* **1999**, *200*, 1722-1725.
- (97) Kim, I.; Hwang, J. M.; Lee, J. K.; Ha, C. S.; Woo, S. I. *Macromol. Rapid Commun.* **2003**, *24*, 508-511.
- (98) Liu, J. Y.; Zheng, Y.; Li, Y. S. *Polymer* **2004**, *45*, 2297-2301.
- (99) Stibrany, R. T.; Schulz, D. N.; Kacker, S.; Patil, A. O.; Baugh, L. S.; Rucker, S. P.; Zushma, S.; Berluce, E.; Sissano, J. A. *Macromolecules* **2003**, *36*, 8584-8586.
- (100) Liu, S.; Elyashiv, S.; Sen, A. *J. Am. Chem. Soc.* **2001**, *123*, 12378-12379.
- (101) Gu, B.; Liu, S.; Leber, J. D.; Sen, A. *Macromolecules* **2004**, *37*, 5142-5144.
- (102) Liu, S.; Gu, B.; Rowlands, H. A.; Sen, A. *Macromolecules* **2004**, *37*, 7924-7929.
- (103) Carlini, C.; Martinelli, M.; Raspolli Galletti, A. M.; Sbrana, G. *Macromol. Chem. Phys.* **2002**, *203*, 1606-1613.
- (104) Frauenrath, H.; Balk, S.; Keul, H.; Höcker, H. *Macromol. Rapid Commun.* **2001**, *22*, 1147-1151.
- (105) Jin, J.; Chen, E. Y. X. *Macromol. Chem. Phys.* **2002**, *203*, 2329-2333.
- (106) Desurmont, G.; Tokimitsu, T.; Yasuda, H. *Macromolecules* **2000**, *33*, 7679-7681.
- (107) The organotitanium-mediated copolymerization of styrene with MMA was however recently reported to occur randomly via a new mechanism consisting of sequential conjugate addition steps. Jensen, T. R.; Yoon, S. C.; Dash, A. K.; Luo, L.; Marks, T. J. *J. Am. Chem. Soc.* **2003**, *125*, 14482-14494.
- (108) Atkins, P. W. *Physical Chemistry*, 5th ed. ; Oxford University Press: Oxford 1994; p 868-869.
- (109) Abu-Surrah, A. S.; Lappalainen, K.; Piironen, U.; Lehmus, P.; Repo, T.; Leskelä, M. *J. Organomet. Chem.* **2002**, *648*, 55-61.
- (110) Griffiths, E. A. H.; Britovsek, G. J. P.; Gibson, V. C.; Gould, I. R. *Chem. Commun.* **1999**, 1333-1334.
- (111) Deng, L.; Margl, P.; Ziegler, T. *J. Am. Chem. Soc.* **1999**, *121*, 6479-6487.
- (112) Bochmann, M.; Lancaster, S. J. *Angew. Chem., Int. Ed. Engl.* **1994**, *33*, 1634-1637.
- (113) Tritto, I.; Donetti, R.; Sacchi, M. C.; Locatelli, P.; Zannoni, G. *Macromolecules* **1997**, *30*, 1247-1252.
- (114) Petros, R. A.; Norton, J. R. *Organometallics* **2004**, *23*, 5105-5107.
- (115) Talsi, E. P.; Babushkin, D. E.; Semikolenova, N. V.; Zudin, V. N.; Panchenko, V. N.; Zakharov, V. A. *Macromol. Chem. Phys.* **2001**, *202*, 2046-2051.

-
- (116) Bryliakov, K. P.; Semikolenova, N. V.; Zudin, V. N.; Zakharov, V. A.; Talsi, E. P. *Catal. Commun.* **2004**, *5*, 45-48.
- (117) Bryliakov, K. P.; Semikolenova, N. V.; Zakharov, V. A.; Talsi, E. P. *Organometallics* **2004**, *23*, 5375-5378.
- (118) Britovsek, G. J. P.; Cohen, S. A.; Gibson, V. C.; van Meurs, M. *J. Am. Chem. Soc.* **2004**, *126*, 10701-10712.
- (119) Whitehouse, C. M.; Dreyer, R. N.; Yamashita, M.; Fenn, J. B. *Anal. Chem.* **1985**, *57*, 675-679.
- (120) Fenn, J. B.; Mann, M.; Meng, C. K.; Wong, S.F.; Whitehouse, C. M. *Science* **1989**, *246*, 64-71.
- (121) Vestal, M. L. *Chem. Rev.* **2001**, *101*, 361-375.
- (122) Lipshutz, B. H.; Stevens, K. L.; James, B.; Pavlovich, J. G. *J. Am. Chem. Soc.* **1996**, *118*, 6796-6797.
- (123) Aliprantis, A. O.; Canary, J. W. *J. Am. Chem. Soc.* **1994**, *116*, 6985-6986.
- (124) Sabino, A. A.; Machado, A. H. L.; Correia, C. R. D.; Eberlin, M. N. *Angew. Chem. Int. Ed.* **2004**, *43*, 2514-2518.
- (125) Feichtinger, D.; Plattner, D. A.; Chen, P. *J. Am. Chem. Soc.* **1998**, *120*, 7125-7126.
- (126) Chen, P. *Angew. Chem. Int. Ed.* **2003**, *42*, 2832-2847.
- (127) Hinderling, C.; Chen, P. *Angew. Chem. Int. Ed.* **1999**, *38*, 2253-2256.
- (128) The *m/z* value found in literature for $3\cdot\text{CH}_3\text{CN}$, SbF_6^- measured by FAB mass spectrometry is 572 amu; see reference 24.
- (129) The MAO/Fe ratio was voluntarily limited to 50 in order to avoid the occlusion of the ESI injector by the formation of aluminum oxide, and to avoid the contamination of the detector with TMA oligomers. This relatively low MAO/Fe ratio explains the presence of $[\mathbf{1}\text{-Cl}]^+$ as one of the activation products.
- (130) Jordan, R. F.; Dasher, W. E.; Echols, S. F. *J. Am. Chem. Soc.* **1986**, *108*, 1718-1719.
- (131) Jordan, R. F.; Bajgur, C. S.; Willett, R.; Scott, B. *J. Am. Chem. Soc.* **1986**, *108*, 7410-7411.
- (132) Jordan, R. F.; LaPointe, R. E.; Bradley, P. K.; Baenziger, N. *Organometallics* **1989**, *8*, 2892-2903.
- (133) Coevoet, D.; Cramail, H.; Deffieux, A. *Macromol. Chem. Phys.* **1996**, *197*, 855-867.
- (134) Coevoet, D.; Cramail, H.; Deffieux, A. *Macromol. Chem. Phys.* **1998**, *199*, 1451-1457.
- (135) Fiedler, A.; Schröder, D.; Scharwz, H.; Tjelta, B. L.; Armentrout, P. B. *J. Am. Chem. Soc.* **1996**, *118*, 5047-5055.

-
- (136) Kirkwood, D. A.; Stace, A. J. *Int. J. Mass Spectrom. Ion Processes* **1997**, *171*, 39-49.
- (137) Kaminsky, W.; Strübel, C. *J. Mol. Catal. A: Chem.* **1998**, *128*, 191-200.
- (138) Kaminsky, W.; Steiger, R. *Polyhedron* **1988**, *7*, 2375-2381.
- (139) Additionally, interactions between Cp_2ZrMe^+ and TMA were observed in the gas phase by Fourier transform ion cyclotron resonance mass spectroscopy; see Siedle, A. R.; Newmark, R. A.; Schroepfer, J. N.; Lyon, P. A. *Organometallics* **1991**, *10*, 400-404.
- (140) Babik, S. T.; Fink, G. *J. Mol. Catal. A: Chem.* **2002**, *188*, 245-253.
- (141) Bart, S. C.; Hawrelak, E. J.; Schmisser, A. K.; Lobkovsky, E.; Chirik, P. J. *Organometallics* **2004**, *23*, 237-246.
- (142) Vela, J.; Vaddadi, S.; Cundari, T. R.; Smith, J. M.; Gregory, E. A.; Lachicotte, R. J.; Flaschenriem, C. J.; Holland, P. L. *Organometallics* **2004**, *23*, 5226-5239.
- (143) Hermes, A. R.; Girolami, G. S. *Organometallics* **1987**, *6*, 763-768.
- (144) Ikariya, T.; Yamamoto, A. *J. Chem. Soc., Chem. Commun.* **1974**, 720.
- (145) Ikariya, T.; Yamamoto, A. *J. Organomet. Chem.* **1976**, *118*, 65-78.
- (146) Haddleton, D. M.; Crossman, M. C.; Hunt, K. H.; Topping, C.; Waterson, C.; Suddaby, K. G. *Macromolecules* **1997**, *30*, 3992-3998.
- (147) Nagel, M.; Paxton, W. F.; Sen, A.; Zakharov, L.; Rheingold, A. L. *Macromolecules* **2004**, *37*, 9305-9307.
- (148) Braunstein, P.; Frison, C.; Morisse, X. *Angew. Chem. Int. Ed.* **2000**, *39*, 2867-2870.
- (149) Resconi, L.; Cavallo, L.; Fait, A.; Piemontesi, F. *Chem. Rev.* **2000**, *100*, 1253-1345.
- (150) Suchopárek, M.; Spěváček, J. *Macromolecules* **1993**, *26*, 102-106.
- (151) Hayen, A.; Koch, R.; Saak, W.; Haase, D.; Metzger, J. O. *J. Am. Chem. Soc.* **2000**, *122*, 12458-12468.
- (152) Peruch, F.; Cramail, H.; Deffieux, A. *Macromolecules* **1999**, *32*, 7977-7983.
- (153) Jin, J.; Mariott, W. R.; Chen, E. Y. X. *J. Polym. Sci. Part A: Polym. Chem.* **2003**, *41*, 3132-3142.
- (154) Ystenes, M. *Makromol. Chem., Macromol. Symp.* **1993**, *66*, 71-82.
- (155) Fait, A.; Resconi, L.; Guerra, G.; Corradini, P. *Macromolecules* **1999**, *32*, 2104-2109.
- (156) Richardson, D. E.; Alameddini, G. N.; Ryan, M. F.; Hayes, T.; Eyler, J. R.; Siedle, A. R. *J. Am. Chem. Soc.* **1996**, *118*, 11244-11253.
- (157) Odian, G. *Principles of Polymerization*, 3rd ed.; Wiley: New York 1991; p 217-219, p 222 and references therein.

-
- (158) A pale blue solution was obtained, exhibiting a UV-Vis spectrum fairly similar to the initial spectrum of **1**, attributed to the bis-enolate product **7'**.
- (159) The reaction product of MAO activated 2,6-bis(imino)pyridine iron(II) chloride complexes with ethanol, seemingly a diethoxy iron complex, was reported to give a UV-vis spectrum similar to the original dichloride complex; see Luo, H. K.; Yang, Z. H.; Mao, B. Q.; Yu, D. S.; Tang, R. *G. J. Mol. Catal. A: Chem.* **2002**, *177*, 195-207.
- (160) When **4** was directly reacted with the dimethylanilinium borate compound, a unique absorption at 605 nm was detected, obviously arising from a monochloride cationic iron complex bearing the borate counter-anion.
- (161) Ethyl acrylate was recently reported to bound to a cationic three-coordinated iron(II) complex via its carbonyl oxygen; see Gregory, E. A.; Lachicotte, R. J.; Holland, P. L. *Organometallics* **2005**, *24*, 1803-1805.
- (162) It is likely that in **7**, the iron atom coordinates with *tert*-butyl propionate, product of the reaction with the borate activator.
- (163) Gaddam, N. B.; Newmark, R. A.; Chien, J. C. W. *Macromolecules* **1994**, *27*, 3383-3388.
- (164) Yamamoto, A. *J. Chem. Soc., Dalton Trans.* **1999**, 1027-1037.
- (165) Yang, P.; Chan, B. C. K.; Baird, M. C. *Organometallics* **2004**, *23*, 2752-2761.
- (166) Schaper, F.; Foley, S. R.; Jordan, R. F. *J. Am. Chem. Soc.* **2004**, *126*, 2114-2124.
- (167) Li, Z.; Goff, H. M. *Inorg. Chem.* **1992**, *31*, 1548-1550.
- (168) Goff, H. M.; Song, B. *Inorg. Chem.* **1994**, *33*, 5979-5980.
- (169) Riordan, C. G.; Halpern, J. *Inorg. Chim. Acta* **1996**, *243*, 19-24.
- (170) Kisko, J. L.; Hascall, T.; Parkin, G. *J. Am. Chem. Soc.* **1998**, *120*, 10561-10562.
- (171) Stuhldreier, T.; Keul, H.; Höcker, H. *Organometallics* **2000**, *19*, 5231-5234.
- (172) Rodriguez-Delgado, A.; Mariott, W. R.; Chen, E. Y. X. *Macromolecules* **2004**, *37*, 3092-3100.
- (173) Tian, G.; Boyle, P. D.; Novak, B. M. *Organometallics* **2002**, *21*, 1462-1465.
- (174) Braunstein, P.; Frison, C.; Morise, X. *Angew. Chem. Int. Ed.* **2000**, *39*, 2867-2870.
- (175) M. Iwamoto, S. Yuguchi, *J. Org. Chem.*, **1966**, *31*, 4290-4291.
- (176) R. Po, N. Cardi, R. Santi, A. M. Romano, C. Zannoni, S. Spera, *J. Polym. Sci: Part A: Polym. Chem.*, **1998**, *36*, 2119.
- (177) C. Janiak, P. G. Lassahn, *Macromol. Rapid. Commun.*, **2001**, *22*, 479-492.
- (178) Y. Jang, P. Kim, H. Lee, *Macromolecules*, **2002**, *35*, 1477-14480.
- (179) D. Nečas, M. Kotora, I. Císařová, *Eur. J. Org. Chem.*, **2004**, 1280-1285.